
Document Number**:** H2020-ICT-52/RISE-6G/D5.1

Project Name:
**R**econfigurable **I**ntelligent **S**ustainable **E**nvironments for **6G** Wireless Networks
(RISE-6G)

# Deliverable D5.1

# Control for RIS-based localisation and sensing (Intermediary Specifications)


| | | | |
|---|---|---|---|
| Date of delivery: | 30/04/2022 | Version: | 2.0 |
| Start date of Project: | 01/01/2021 | Duration: | 36 months |


# Deliverable D5.1

## Control for RIS-based localisation and sensing (Intermediary Specifications)

| | |
|---|---|
| **Project Number**: | 101017011 |
| **Project Name:** | **R**econfigurable **I**ntelligent **S**ustainable **E**nvironments for **6G** Wireless Networks |

| | |
|---|---|
| **Document Number**: | H2020-ICT-52/RISE-6G/D5.1 |
| **Document Title:** | Control for RIS-based localisation and sensing (Intermediary Specifications) |
| **Editor(s):** | Henk Wymeersch (CHA) |
| **Authors:** | Henk Wymeersch (CHA), Benoit Denis (CEA), George Alexandropoulos (NKUA), Petar Popovski (AAU), Kimmo Kansanen (AAU), Vincenzo Sciancalepore (NEC), Radoslaw Kotaba (AAU), Kamran Keykhosravi (CHA), Musa Furkan Keskin (CHA), Ioanna Vinieratou (NKUA), Moustafa Rahal (CEA) |
| **Dissemination Level:** | PU |
| **Contractual Date of Delivery:** | 30/04/2022 |
| **Security:** | Public |
| **Status:** | Final |
| **Version:** | 2.0 |
| **File Name:** | RISE-6G_WP5_D5.1_Final.docx |



**Abstract**

This deliverable provides the results of the RISE-6G proposals on architectures, control, signalling, and data flow related to work package 5 “RIS for Enhanced Localisation and Sensing”, as well as initial performance evaluations of these proposals.

**Keywords**

*Beyond-5G; 6G; RIS; Localisation; Sensing.*

# Contents

# List of Figures

# List of Tables

# List of Acronyms

| | |
|---|---|
| **5G-NR** | 5th Generation - New Radio |
| **AMF** | Access and Mobility management Function |
| **BS** | Base Station |
| **CAPEX** | CAPital EXpenditure |
| **CSI** | Channel state information |
| **DL** | Downlink |
| **DL-DoD** | Downlink Direction of Departure |
| **DL-TDoA** | Downlink Time Difference of Arrival |
| **DoA** | Direction of Arrival |
| **DoD** | Direction of Departure |
| **EM** | Electromagnetic |
| **FF** | Far-field |
| **FIM** | Fisher information matrix |
| **FMCW** | Frequency Modulated Continuous Wave |
| **GDoP** | Geometric Dilution of Precision |
| **KPI** | Key-Performance Indicator |
| **LB-AoI** | Localization Boosted - Area of Influence |
| **LE-AoI** | Localization Enabled - Area of Influence |
| **LMF** | Location Management Function |
| **LoS** | Line-of-Sight |
| **LTE** | Long Term Evolution |
| **MC** | Multicarrier |
| **MIMO** | Multiple Inputs Multiple Outputs |
| **NF** | Near-field |
| **NLoS** | Non-line-of-sight |
| **NVAA** | Non-Value-Added Activities |
| **OFDM** | Orthogonal Frequency Division Multiplexing |
| **OPEX** | OPerating EXpenditure |
| **PEB** | Position error bound |
| **RF** | Radio Frequency |
| **R-RIS** | Reflective RIS |
| **RT-RIS** | Reflective-transmission RIS |
| **RIS** | Reconfigurable Intelligent Surface |
| **RISC** | RIS controller |
| **RISO** | RIS orchestrator |
| **RSSI** | Received Signal Strength Indicator |
| **RTT** | Round Trip Time |
| **RT-ToF** | Round Trip – Time of Flight |
| **Rx** | Receiver |
| **SISO** | Single Input Single Output |
| **SLAM** | Simultaneous Localisation and Mapping |
| **SNR** | Signal-to-noise ratio |
| **TDoA** | Time Difference of Arrival |
| **ToA** | Time of Arrival |
| **Tx** | Transmitter |
| **UAV** | Unmanned Aerial Vehicle |
| **UE** | User |
| **UTDoA** | Uplink Time Difference of Arrival |
| **UL** | Uplink |
| **UL-DoA** | Uplink Direction of Arrival |
| **UL-TDoA** | Uplink Time Difference of Arrival |
| **WP** | Work package |

# 1 Introduction

The RISE-6G project is one of the 5G-PPP projects under the European Commission's Horizon 2020 framework. The focus of the project is to design, prototype, and trial radical technological advances based on reconfigurable intelligent surfaces (RISs) to forge a new generation of dynamically programmable wireless propagation environments. RISs will both enable and boost connectivity, localisation, and sensing performance, as well as adapt to dynamic requirements on electromagnetic field emissions, energy efficiency, and secrecy.
Within RISE-6G, work package 5 (WP5) considers exploiting RIS for improved localisation, sensing and mapping performances. The aim of WP5 is two-fold: (i) to develop localisation-oriented network architecture for RIS deployment and profile control to optimise the aforementioned features' key performance indicators (KPIs); (ii) to develop and evaluate detection and estimation algorithms that enable RIS-based localisation and sensing, for localisation devices, building dynamic environments and radio maps as well as passive sensing.

## 1.1 Deliverable objectives

This document provides the intermediate results related to the first aim and covers different KPIs, architectural alternatives, RIS control strategies, as well as data flow and signalling, derived from the various contributions within WP5. These results serve as input for the work in WP2 on architectures, deployment strategies, and RIS control.

As RISE-6G Project targets very different objectives in WP4, WP5, WP6, the following two-step approaches has been chosen, to derive architecture and control signalling requirements:

- During step 1: each WP derives its initial views on requirements on architecture and signalling, based on the WP very specific objectives and the WP's list of technical contributions and innovations; the results of these independent works are reported in D4.1, D5.1 and D6.1, separately.
- During step 2: WP2 uses D4.1, D5.1 and D6.1 as inputs to build a common framework for architecture and control signalling that will be described in D2.5.

Consequently, concepts and vocabulary regarding architecture and control signalling may differ in D4.1, D5.1 and D6.1. The name "RIS controller" for instance, may have a slightly different meaning in two different deliverables. However, it will be clearly defined inside each deliverable. Common concepts and vocabulary which will be defined in D2.5, to be used afterwards during the project.

## 1.2 Deliverable structure

The rest of the document has the following structure. Section 2 reviews the basics of localisation and sensing, contrasting conventional approaches without RIS and envisions approaches with RIS. The section also motivates the need for suitable architectures and control. The relevant KPIs are described in Section 3, along with methods for evaluating them. Section 4 details six architectural alternatives proposed in RISE-6, starting from a baseline architecture with a single RIS, a BS, and a single UE. In parallel, Section 5 details six RIS control approaches, which determine the RIS configurations needed for supporting localisation and sensing. As will be apparent, both the architectures and control approaches can take on a variety of forms and are in general different from those needed to support communication. To further emphasise this point, Section 6 describes the signal flow and timeline for each of the architectural and control alternatives. Finally, Section 7 concludes the deliverable with recommendations for the overall RISE-6G architecture.

# 2 Localisation and sensing

The purpose of this section is to provide a brief overview of the principles of radio localisation and sensing, with an emphasis of cellular approaches. Then the general use of RISs in the context of localisation and sensing will be detailed, followed by a discussion on the corresponding need for architectures and control methods. It should be noted that localisation relies on sensing to provide measurements of angles and

delays. Hence, while the focus of this deliverable is mainly on localisation, it also inherently extends to sensing.

## 2.1 Foundations of localisation

In the context of radio systems, localisation (synonym: positioning) is the process of determining the 2D or 3D location of a connected device (a user equipment (UE)), based on uplink (UL) or downlink (DL) measurements with respect to several base stations (BSs) [PRL+18]. The measurements are performed based on the reception of dedicated pilot signals and can be of the forms described in Table 2-1. Observe that a combination of angle and delay measurements can be used for UE localisation and that different measurement combinations put different requirements on both the number of BSs as well as on their mutual synchronisation. For this latter reason, pure ToA measurements with a UE synchronized to a BS is impractical in real scenarios, since even small synchronisation errors lead to large localisation errors (e.g., 10 ns clock error corresponds to 3 meters error). Examples of two different measurement for localisation are shown in Figure 2-1.

**Table 2-1. Localisation measurements and requirements for 3D positioning.**

| Measurement | UL or DL | Number of BSs needed | Comment |
|---|---|---|---|
| Time-of-arrival (ToA) of the first path | Either | 3 | BSs should be synchronized with the UE |
| Time-difference-of-arrival (TDoA), derived from several ToA measurements | Either | 4 | BSs should be mutually synchronized |
| Round-trip-time (RTT), derived from several ToA measurements | Both | 3 | No synchronisation needed |
| Angle-of-arrival (AoA) at the BS | UL | 2 | Requires planar arrays at each BS |
| Angle-of-departure (AoD) from the BS | DL | 2 | Requires planar arrays at each BS |
| TDoA+UL-AoA | UL | 2 | BSs should be mutually synchronized |
| RTT+ UL-AoA | Both | 1 | No synchronisation needed |

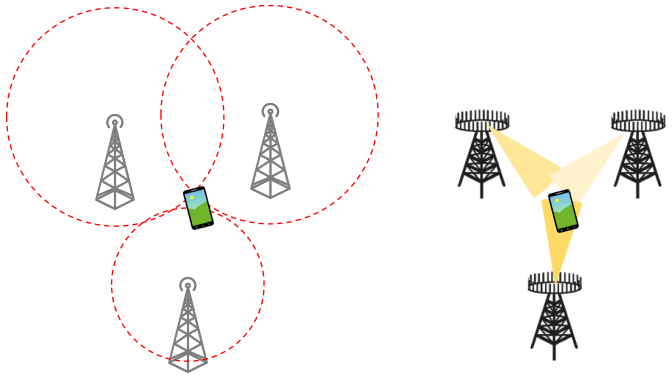

**Figure 2-1. Example of RTT-based localisation (left), constraining the UE on the intersection of circles (2D) or spheres (3D); and localisation based on DL-AoD measurements (right), constraining the user within a sector of each BS.**

The pilots used for localisation are tailored in time, frequency, and space. In time-frequency, so-called comb signals are used, which occupy the entire signal bandwidth while allowing orthogonality across BSs [3gpp10]. In space, the time-frequency signals are repeated for different directional beams at the BS, while providing angle measurements (AoA in UL or AoD in DL). The quality of the ToA and AoA/AoD measurements depends on several factors [WLW+18]:

- **Bandwidth:** the amount of available bandwidth is directly related to delay resolution and thus to multipath suppression (in particular, two paths can be resolved if their delay difference is at least 1 over the bandwidth). If strong signal paths are present, say, 10 meters after the direct path, then a bandwidth of around 30 MHz is needed to resolve this secondary path. For that reason, a large bandwidth is important for accurate localisation in cluttered environments.
- **Transmission power:** the accuracy of delay and angle measurements depends on the received signal-to-noise ratio (SNR), which is itself proportional to the transmission power. Hence, higher transmit powers lead to more accurate localisation, provided multipath can be resolved. Since localisation depends on pilot signals, an increase in SNR can also be achieved through longer transmission times.
- **Number of antennas:** similar to bandwidth being related to delay resolution, so is the number of antennas proportional to angle resolution (the relation for a linear array is that two paths with angle difference (in radians) beyond 2/(number of antennas) can be resolved). Hence, a larger array of half-wavelength spaced elements leads to improved angular resolution.
- **Signal processing and hardware limitation:** depending on the computational capacity and knowledge regarding the utilised beams, the delay and angle estimation performance can be improved. Moreover, hardware and calibration errors (e.g., synchronisation errors) significantly affect localisation performance, leading to a significant gap between theory and practice.

In terms of architecture and signalling in 5G [DSM+21], the location management function (LMF) is central, as it configures the UE using the long-term evolution (LTE) positioning protocol and coordinated with the BS. Hence, positioning involves additional control overhead, via the access and mobility management function (AMF), between the LMF, BSs, and UE, as shown in Figure 2-2.

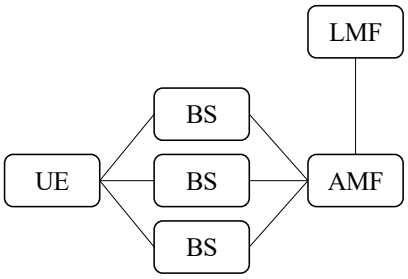


**Figure 2-2. Schematic of 5G positioning architecture, based on [DSM+21], supporting both UL and DL measurements.**

## 2.2 Foundations of sensing

Sensing in general involves the detection and estimation of changes or events in the environment, including for use in positioning. In radio systems, sensing is often limited to radar-like sensing, i.e., detection and tracking of passive objects. In contrast to localisation, 3GPP has until now not offered any support for radar-like sensing. Such sensing is conventionally broken down as [WSD+21]:

- **Monostatic sensing:** a transmitter (Tx) and receiver (Rx) are co-located and share a common clock. The Tx emits a waveform, known to the Rx. The Rx processes the backscattered waveform to detect the presence of targets (static or dynamic object), as well as their distance, bearing, and velocity. Such type of radar sensing is commonly employed in automotive radar, and requires dedicated waveforms, shaped in time and frequency (e.g., frequency modulated continuous wave (FMCW) [LLH+16] [SFS+18]) with orthogonality across transmit antennas, to provide a large virtual aperture. FMCW-type waveforms have a constant envelope, making them hardware-friendly. In the context of communication systems, standard data-bearing signals can be used (e.g., orthogonal frequency division multiplexing (OFDM)) [CKA+20]. Monostatic sensing requires a full-duplex receiver.

- **Bistatic sensing:** now, Tx and Rx need not be co-located and don't share a common clock. Pilot signals are emitted by the Tx and the backscattered signal is processed by the Rx. The lack of synchronisation requires a clock reference, which can be offered by the direct path between Tx and Rx.
- **Multistatic sensing:** this is a generalisation of bistatic sensing with several Rx. The information for the different Rx must be fused to provide an overall picture of the detected objects. The larger number of Rx allows for higher resolution, due to the increased aperture, provided the Rx are synchronized.

The discussion related to delay and angle resolution, as well as signal processing and hardware limitations from Section 2.1 is still relevant. In terms of power, it is important to note that sensing is subject to more severe path loss than localisation, as the signal scatters from objects before reaching the Rx.

## 2.3 RIS in localisation and sensing

RISs have the potential to improve localisation and sensing performance, when added to conventional deployments [WHD+20]. This is referred to as 'boosting'. In addition, RIS also have the potential to provide location estimates to UEs when conventional deployments fail. This is referred to as 'enabling'.

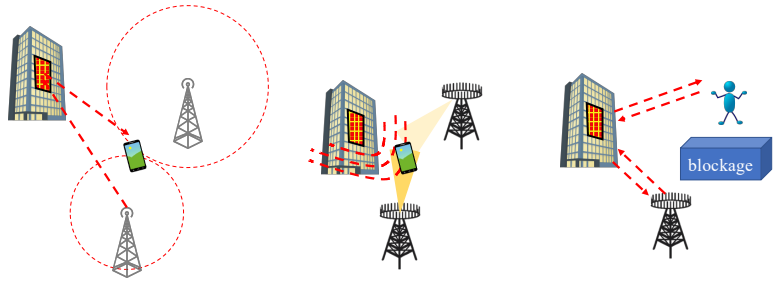


**Figure 2-3. Examples of use of RIS in localisation: a new signal path via a RIS and a new reference by the RIS (left); large RIS provides wavefront curvature for localisation measurements (middle); a RIS provides a signal path to avoid signal blockage in monostatic sensing.**

In wireless systems, RISs can boost or enable user localisation by providing the following (see Figure 2-3):

1. **New signal path**: The reflected signal from the RIS provides the Rx with an additional signal path whose parameters can be estimated and used for localisation. Compared to other multipath generated by the scatterers, the path from the RIS is stronger due to multitude of RIS elements and beamforming gain.
2. **New location references**: RISs, when used as a part of wireless infrastructure, have a fixed location and orientation. Therefore, they provide a location reference that can be used to estimate the unknown location of the user. This separates RISs from scatterers in the environment as the locations of the scatterers are often unknown.
3. **Near-field measurements:** Since the dimensions of RISs are much larger than the conventional planar arrays used in MIMO systems, and they can be installed close to the user site, it is probable that the user falls within the near-field of the RIS [DNA+21]. In the near-field, one can also use the phase of the received signal to estimate the location of the user.

Table 2-2 presents some of the scenarios where the user localisation in 3D is possible for wireless systems equipped with RISs. Here only single-antenna BSs is considered.

**Table 2-2 RIS Localisation measurements and requirements for 3D positioning.**

| Measurement | UL or DL | # BSs | #RISs |
|---|---|---|---|
| ToA + AoD | Both | 0 | 1 |
| TDoA + AoD | Either | 1 | 1 |
| AoD | Either | 1 | 2 |

### 2.4 Need for architectures and control

RIS is a new network element and its integration into the network infrastructure requires a structured approach that defines both the roles of the RIS as well as the protocols between the RIS and the rest of the system [DZD+20]. The RIS phase configuration controls the physical observation that positioning is based on, and thereby any positioning strategy either requires the explicit control of the RIS configuration or must operate with the knowledge of the RIS configuration in use. The architecture must consider that the RIS is envisioned as a multi-purpose element, used for communication, sensing, and positioning. The required architecture is envisioned to include the following components:

- **RIS:** is the reflect-array or meta-material device that is directly controlled by an associated RISC. Expected time granularity between 100 microseconds and 10 ms. Advanced configuration may place the RIS (logically) connected to CU/DU of 3GPP RAN architecture. Interfaces and reference points are to be further clarified in future deliverables.
- **RIS controller (RISC):** the controller associated to a single RIS device. The controller can be part of the RAN element or directly interact with a RAN element (gNb or eNb in 3GPP jargon). In addition, it may directly interact with O-RAN near-RT RIC. Expected time granularity: 10-50 ms.
- **RIS orchestrator (RISO):** the orchestrator is placed on a higher (hierarchical) layer and orchestrate multiple RIS-Cs and/or RAN elements. It can directly interact with 3GPP AMF, ETSI MEC orchestrator or ETSI NFV orchestrator. Time granularity is expected between 100 ms – a few seconds.

## 3 Key performance indicators, methods, and evaluation

### 3.1 Localisation and sensing performance metrics

In this subsection, recall the generic metrics and indicators initially introduced in Deliverable 2.4 [RISE6GD2.4] to assess the performance of RIS-based localisation and sensing. As already suggested above, the *sensing* functionality shall be intended here as the *localisation of passive entities* (i.e., non-connected objects or non-cooperative devices), in contrast to the active localisation of connected devices, which is simply depicted as *localisation*. Accordingly, all the localisation-oriented metrics detailed below would still hold for the evaluation of sensing performances. Additional metrics can be found in the literature, e.g., [ZGL19].

#### 3.1.1 Localisation accuracy

Accuracy is fundamentally determined by the statistics of the 3D localisation error $\mathbf{e} = \mathbf{x} - \hat{\mathbf{x}}$, which represents the deviation of an estimate $\hat{\mathbf{x}}$ from a Ground-Truth location $\mathbf{x}$. This error is usually seen as a random variable comprising both horizontal (XY) and vertical (Z) error components. Accuracy is arguably the most relevant and definitive metric to characterize any localisation method, as it intrinsically accounts for several -and likely combined- factors, such as received signal-to-noise-ratio (SNR), resolution capabilities (i.e., the separability of correlated received radio signals) and state identifiability (i.e., the existence of a continuous or discrete set of possible solutions, depending on both connectivity conditions and network deployment geometry). Relevant statistics characterizing the 3D or 2D localisation errors include e.g.,

- **Mean Square Error (MSE):** $\mathbb{E}[\mathbf{e}^T\mathbf{e}]$;
- **Root MSE (RMSE):** $\sqrt{\mathbb{E}[\mathbf{e}^T\mathbf{e}]}$ ;
- **Accuracy (with confidence level α ):** $e: p(\|\mathbf{e}\| < e) = \alpha$;
- **Horizontal accuracy (with confidence level α ):** $e: p(\|\mathbf{e}_{1:2}\| < e) = \alpha$;
- **Vertical accuracy (with confidence level α ):** $e: p(|e_3| < e) = \alpha$.

The evaluation of accuracy levels typically relies on the cumulative distribution function (CDF) of the localisation estimation error, which can reflect more accurately effects such as heavy-tailed/asymmetric

localisation error distributions, beyond more "compact" indicators such as MSE. Alternative metrics such as the circular error probability (CEP) or the hit target radius (HTR) can also be considered. CEP is defined as the probability for a location estimate to fall into a circle (resp. sphere) of radius $R$ centred around the ground-truth location in 2D (resp. 3D). HTR corresponds to CEP equal to 50%.

### 3.1.2 Localisation-related delays

As localisation is often time-sensitive and sometimes safety-critical, there are also specific localisation-related delay metrics that impact the reactivity of the localisation system, as well as its capability to cope with mobility (typically from a tracking standpoint in the steady state regime), namely.

- **First time to fix (seconds)**: time until the system provides the first location estimate.
- **Localisation latency (seconds):** time between a positioning request and the position being available.
- **Update rate (Hz)**: frequency of successive position estimates.

### 3.1.3 Localisation integrity

In certain critical applications, the localisation error cannot exceed certain safe thresholds and the localisation service must be available without interruption. Relevant metrics in this regard are:

- **Reliability:** measured by mean-time between failures (MTBF) or duration of the time the service is available.
- **Availability:** fraction of the time the service is available.

High reliability means high availability, but not the other way around. Hence, a system that is down (i) every other minute for 1 minute or (ii) every other hour for 1 hour has the same availability, but very different reliability.

**Table 3-1 Main performance metrics.**

| Metric | Unit | Example | Comments |
|---|---|---|---|
| Location accuracy | Meter | 1 meter accuracy with 95% confidence | Accounts for both biases and variance (precision and accuracy). |
| Latency | Seconds | 10 ms | Includes control and signalling overhead, signal transmission time, and signal processing. |
| Update rate | Hertz | 1 Hz | Bounded by the latency. |
| Reliability | Seconds | A MTBF of 50 hours means that the system on average works for 50 hours until a failure occurs | Depends mainly on uptime of base stations and user devices. |
| Availability | % or fraction of time | 99.99% or 23.9976 hours in 24 hours. | Depends also on deployments, and uncontrolled factors (e.g., environment). |

## 3.2 Methods and evaluation

Based on the previous metrics and indicators, the chosen methodology to practically assess the performance of the proposed RIS control mechanisms and/or RIS-enabled system architecture in the RISE-6G project is based on both numerical simulations (incl. theoretical performance bounds evaluations) and real experimental data (i.e., either by emulating the system offline, or through real-time demonstrations). Although both aspects are developed in this subsection for the sake of completeness, the focus of this deliverable is put on the former simulation-based evaluations.

### 3.2.1 Theoretical bounds

First, theoretical performance bounds are used to provide strong guarantees on both the optimality and the reliability of the proposed RIS-enabled localisation solutions. Typically, the position error bound (PEB) is a theoretical tool accounting for the best localisation accuracy achievable by any unbiased estimator, assuming a priori statistics for the measured radio signals (or for radio metrics estimated out of received signals) used as observations, as well as the knowledge of user's and BSs' locations. The PEB is defined from the Fisher information matrix **J**, which represents a theoretical lower bound on the error covariance, as follows:

$$\mathbf{J^{-1}(x)} \preccurlyeq \mathbb{E}[(\mathbf{x}-\hat{\mathbf{x}})(\mathbf{x}-\hat{\mathbf{x}})^{\mathbf{T}}].$$

The PEB (expressed in meters) at a location **x** is then calculated as

$$\mathbf{PEB(x)} = \sqrt{\mathbf{trace}\left(\mathbf{J^{-1}(x)}\right)} \leq \sqrt{\mathbb{E}[\|\mathbf{x}-\hat{\mathbf{x}}\|^{\mathbf{2}}]}.$$

Given any concrete scenario under test (i.e., simulated, or experimental), the PEB can hence be numerically evaluated as a function of key system parameters (e.g., SNR per radio link, operating frequency, bandwidth, etc.) and the true locations of all the physical entities involved in the localisation problem (incl. that of the user or objects to be positioned).

Note that there exists a variety of bounds to the achievable accuracy apart from the well-known Cramer-Rao bound described above, such as the Weiss-Weinstein bound or the Ziv-Zakaï bound, which are typically more suitable at low SNR regimes.

Finally, to assess uniquely the effect of network deployment geometry (i.e., user's relative position with respect to BSs) regardless of SNR conditions, one can evaluate the geometric dilution of precision (GDoP) in 2D or 3D, which is somehow already integrated by default in the PEB calculation.

### 3.2.2 Simulations

In simulation-based evaluations, the evaluation of accuracy levels practically relies on the empirical CDF of the localisation estimation error, which is obtained over multiple simulation trials while introducing randomness between these successive trials (e.g., in terms of noise realisations and/or tested positions, etc.), depending on the considered scenario. This empirical CDF is used in practice to characterize characteristic error values. Such critical values include for instance the median error at 50% of the CDF, or so-called "worst case" localisation error at arbitrary high CDF values, typically 90% or 99%, i.e., the critical error value such that 90% or 99% of the localisation errors (over all simulation trials) have a smaller magnitude.

Ideally, the tested localisation methods themselves are also expected to provide a localisation error indicator (e.g., a 90% confidence ellipsoid). The size of this ellipsoid is then interpreted as a reliable measure of the accuracy, as perceived internally by the algorithm (and given that no overconfidence issue has been spotted within the estimation process).

A priori, localisation-related delays are not trivial to assess in absolute values through simulations, given the typically high levels of system abstraction of signal-oriented simulation tools. However, impacting aspects such as overhead or frame durations can at least be covered in more protocol-oriented simulations.

### 3.2.3 Experiments

Evaluations based on experimental data are typically split in two categories depending on the available hardware, namely *offline system emulations* (based on e.g., pieces of metrology equipment such as channel sounders) and quasi *real-time trials* (based on e.g., integrated devices, as close as possible to commercial devices). In both categories, the measurement of the localisation accuracy requires a side **ground-truth referencing system**, whose uncertainty should be at least several orders of magnitude below that of the system under test. This ground-truth system is particularly challenging in dynamic indoor scenarios, so that simplified approaches are often applied (typically, projecting time-stamped localisation estimates onto piece-wise segments of the followed path), at the price of approximations. In static scenarios (i.e., freezing a deployment configuration and for a given position under test), just like in simulation-

based evaluations, the accuracy levels can be simply assessed with the empirical CDF of the localisation estimation error, which is obtained over a sequence of successive measurements.
As for localisation-related delays, they can be measured at the mobile UE or network side, depending on (i) where the location computation takes place, (ii) which system entity requests the location information and (iii) where the latter information must be ultimately issued. The localisation application itself should also provide timestamps of when the measurements were taken, when the location was computed, and when the location was provided to the application.
As the localisation application is supposed to provide an evaluation of the localisation uncertainty (e.g., 90% confidence ellipses or covariances), integrity monitoring (incl. fault detection and exclusion) can be performed externally to the localisation application itself. Practically, one can simply measure how often the actual localisation error exceeds the uncertainty values indicated by the localisation error covariances (i.e., timewise or per attempt), that is, the fraction of instances when the actual error is outside the confidence levels provided by the application's uncertainty estimates.

# 4 Architectures

The architecture envisioned includes two components that are involved in configuring and using the RIS as a system component, a RIS orchestrator and a RIS controller. Here, the focus is on the latter, as it is the RIS controller that executes the instantaneous control actions on the RIS hardware.
In the architecture considerations that follow, the main emphasis is on functionality, information flow, and signalling needs. The outlined architectures are expected to be directly applicable in a single operator case but needing further evaluation in a multi-operator case.
Eventually, the envisioned architecture(s) also need to be evaluated for compatibility with the 3GPP framework.

## 4.1 Localisation perspective

The localisation architecture should support collection of measurements at the BTS and/or UE, RIS configuration during the measurements, as well as synchronisation of these with the transmission of pilots by the BTS or UE. Localisation algorithms typically will require knowledge of (or also control over) the RIS configurations utilised during the measurement, as well as the measurements. Therefore, the localisation algorithms can be envisioned performed in either the RIS controller or the measurement point, whereas other choices for computation execution require both the RIS configuration and measurements as inputs. The outlined architectures in Figure 4-1 implement the requirements listed above, with a relatively simple co-operation between the RIS controller and the AMF in all the cases where the RIS is not operate autonomously.

## 4.2 Sensing perspective

A sensing architecture has one main requirement: it must support collection of measurements in a RIS based system. This may be, as in the current contributions, directly from the RIS, either in sampled or sampled and pre-processed baseband format. If observations at the BTS will be relevant for sensing, they should be supported by the architecture.
In all sensing approaches, the data flow is one way, from UE to the network side. The network side collects the information with the endpoint being at the RIS or RIS controller. The necessary signalling includes only the RIS configuration and related timing control. Again, the outlined architectures in Figure 4-1 implement the requirements listed above, with a relatively simple co-operation between the RIS controller and the AMF.

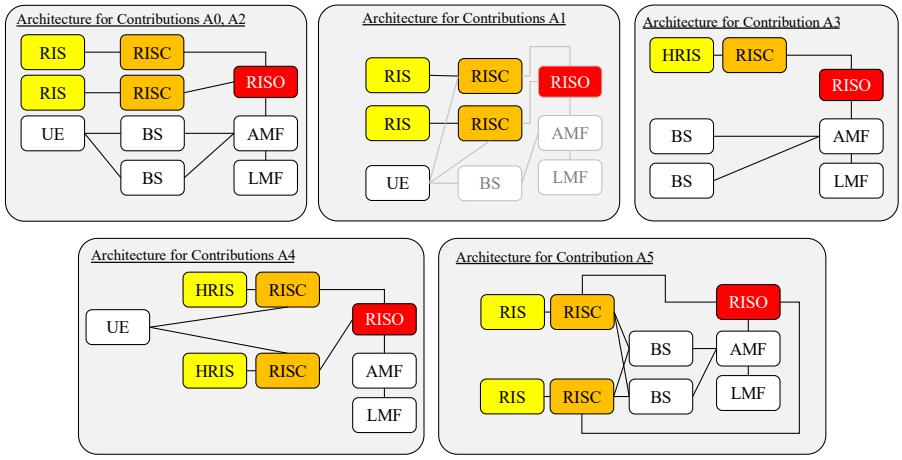


**Figure 4-1 Overview of the RISE-6G localisation and sensing architectures.**

## 4.3 Contributions from RISE-6G

Below, in Table 4-1, the architectural aspects of all RISE-6G localisation and sensing contributions are listed.

**Table 4-1 Overview of the considered architectures for localisation and sensing.**

| **Architecture** | **Con. A-0: RIS-Enabled UE Localisation with Access Points** | **Con. A-1: RIS-Enabled Localisation without Access Points** | **Con. A-2: RIS-Enabled Localisation without Delay-Based Measurements** | **Con. A-3: Receiving RIS to Detect Passive Users** | **Con. A-4: Sensing-RIS-Enabled UE Localisation Without Any Access Points** | **Con. A-5: Mobile RIS localisation** |
|---|---|---|---|---|---|---|
| Nr BS | 1 | 0 | 1 | 1 | 0 | At least 3 |
| Nr RIS | 1 | 1 for RTT and AOD, 3-4 for RTT only | 2 | 1 | 3 | 1 |
| Nr UEs | 1 | 1 | 1 | Multiple | 1 | N/A |
| UE Mobility | Static | Static | Static | Static | Static | Mobile |
| RIS Type | Passive | Passive | Passive | Receiving | Receiving or hybrid | Reflecting |
| Localisation functionality placement | At UE or at BS | At UE | At UE | At RIS | At RIS controller | At BS |
| Nr Operators | 1 | 1 | 1 | 1 | 1 | 1 |
| **Setup** | | | | | | |
| Indoor/outdoor/UAV | Indoor (short range) | Indoor (short range) | Indoor (short range) | Indoor | Indoor | Outdoor |
| 2D/3D | 3D | 3D | 3D | 3D | 3D | 3D |
| Frequency Band | mmWave | mmWave, sub-THz | Any | Sub-6 GHz | Any | Any |
| Near field/far field | Nearfield under LOS blockage. | Far-field | Far-field | Near-field | Far-field | Far-field |
| LOS/NLOS/Both | LOS and NLOS | LOS and NLOS | LOS | LOS and NLOS | LOS and NLOS | LOS and NLOS |
| Imperfections or other hardware considerations | None | Full-duplex UE needed | None | None | None | None |
| **Data flow and signalling** | | | | | | |
| Uplink/Downlink | UL or DL | UL | DL | UL | UL | DL |
| Measurement type | Angle and delay in far-field. Position in near-field | RTT and AOD | AOD | RSS at RIS | AOD at RIS | Delay |
| RIS configuration strategy | Arbitrary or location-based, several profiles needed | Arbitrary or location-based, several profiles needed | Arbitrary or location-based, several profiles needed | Arbitrary phase, quantized phase, finite codebook | Arbitrary, several profiles needed | Random |

| | | | | | | |
|---|---|---|---|---|---|---|
| Who collects measurements | UE or BS | UE | UE | RIS | RIS | BSs |
| Synchronisation | us-level | us-level | us-level | Phase | us-level | Us-level |
| Narrowband/wideband | Wideband. In near-field narrowband is sufficient. | Multi-carrier | Single-carrier | narrowband | narrowband | Wideband |

### 4.3.1 Contribution #A-0: RIS-Enabled UE Localisation with Access Points

#### *4.3.1.1 Motivation and context*

The most canonical way of including RIS in localisation is to consider a standard localisation scenario with one or more users and one or more BSs, with additional RIS. Communication can be in uplink or downlink. The RIS can then boost localisation performance or enable localisation when then infrastructure is not sufficient. In the former case, one can consider 4 BSs using TDOA measurements, enhanced by 1 RIS, providing an additional measurement, provided the RIS location is known. In the latter case, consider the case with a single-antenna BS and a single antenna UE, which is insufficient for localisation. In that case, a RIS provides additional delay and AOD measurements to make the localisation possible, as shown in Figure 4-2 [KKS+21b].

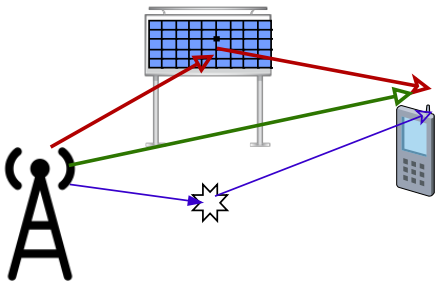

**Figure 4-2: User localisation in a SISO system with one RIS.**

#### *4.3.1.2 Methodology*

Localisation is performed as follows. Only the downlink scenario is considered, while the uplink scenario is similar:

1. The procedure is initiated by the LMF and coordinated by the AMF and RISO.
2. The BS transmits wideband pilots.
3. The RIS reflects these pilots, modulated by individual RIS configurations, generated by the RISC.
4. The UE receives the signal path from the BS, superimposed with the signal path from the RIS.
5. The UE separates the signal path from the RIS, considering zero-mean time-variant encoding at the RIS.
6. The UE estimates the relevant angles and delay from each path and computes its position.

#### *4.3.1.3 Results and outcomes*

Localisation is possible in the minimal scenario from Figure 4-2 [KKS+21b]. Localisation can also be possible when the LOS path between BS and UE is blocked, provided the UE is in near-field to the RIS [RDK+21].

#### *4.3.1.4 Perspective and relation to other WP5 contributions*

This is the canonical localisation setup with a single RIS.

### 4.3.2 Contribution #A-1: RIS-Enabled Localisation without Access Points

#### *4.3.2.1 Motivation and context*

This section introduces a novel structure for user localisation with the help of one RIS and without any access points, presented in [KSA+22]. The architecture consists of one UE and one RIS as shown in Figure 4-3. The UE transmits a wideband signal which is reflected from the RIS. The user then estimates

its location, similarly as in radar systems, by processing the signal that is reflected from the RIS. Systems with joint radar and RIS localisation have been studied previously [BGL+21,LDF+21], however, here use only the signal path from RIS is used to estimate the location. The estimation algorithm is based on a round-trip time (RTT) delay measurements and log-likelihood optimisation. Such architecture can be used in places with no access to any BS such as tunnels and indoor environments.

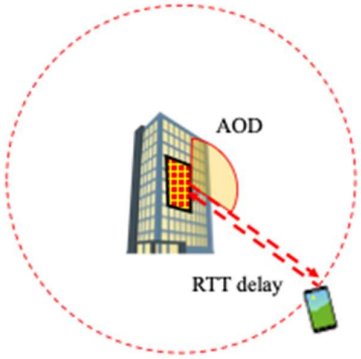


**Figure 4-3 System setup for localisation without any access points using RTT and AOD measurements.**

#### *4.3.2.2 Methodology*

The localisation is performed as follows:

1. First the UE transmits a WB signal to the RIS.
2. Then after modulating the signal phase, the RIS reflects the transmitted signal back to the user, controlled by the RISC.
3. The user receives the signal from the RIS and from the reflectors and scatterers in the environment.
4. The user performs a post processing step to remove the effects of the uncontrolled multipath from the received signal.
5. Finally, the UE estimates the RTT delay as well as the AOD from the RIS and its own location by optimizing the log-likelihood function.

The RIS can act as a UE, in which case the RISC and UE communicate directly. Alternatively, the LMF, AMF, and RISO can be involved.

#### *4.3.2.3 Results and outcomes*

The outcomes of this work are: Introducing a minimal scenario for localisation with only one RIS and no BSs; Developing an estimator with low complexity and developing the CRB lower bounds on the estimation error; Calculating the estimation error and comparing them to the CRB lower bounds. In Figure 4-4, a performance example is shown, indicating that user localisation is indeed possible with high accuracy without any BS. However, due to the large RIS size, wideband beam squint effects may be harmful, when not properly mitigated.

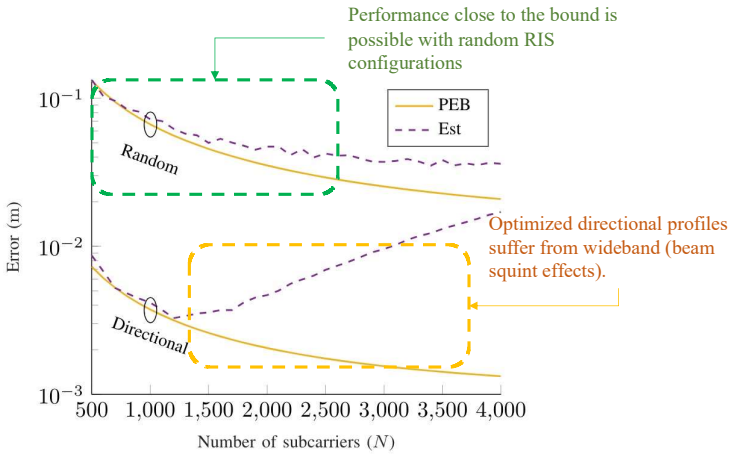


**Figure 4-4 Example of RIS-enabled localisation without a BS [KSA+22].**

#### *4.3.2.4 Perspective and relation to other WP5 contributions*

This section introduces a new RIS-enabled localisation scenario, which can manifest in cases with no nearby access points. In future work, one can consider extensions of this work such as considering RIS impairments, or the user movement effects.

### 4.3.3 Contribution #A-2: RIS-Enabled Localisation without Delay-Based Measurements

#### *4.3.3.1 Motivation and context*

This section looks at a novel scenario, where the user can be localised via two RISs and without any delay measurements. This scenario comprises one BS, two RISs and one or multiple UEs as shown in Figure 4-5. Unlike other RIS-enabled localisation systems such as [KKD+21][KKS+21], here the BS transmits narrow band signals and therefore no delay measurements are possible at the UE. Each UE receives the signal reflected from the two RISs, while the direct channel can be blocked or not. The user location can be estimated from the two angels of departure from the two RISs. This architecture is especially interesting because it eliminates the need for delay measurements and subsequently the need for synchronisation between the infrastructures.

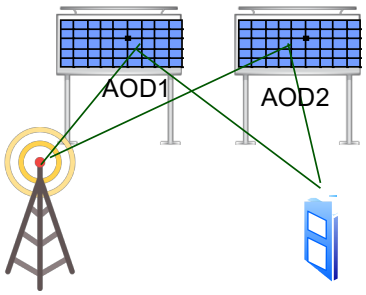


**Figure 4-5: Localisation with two AODs without delay measurements**

#### *4.3.3.2 Methodology*

The localisation is performed as follows:

1. The procedure is initiated by the LMF and coordinated by the AMF and RISO.
2. First the BS transmits a narrow band signal towards the RISs.
3. The RIS reflects the signal, in a manner controlled by the RISC.
4. Next the UE receives the reflected signal from the RISs.

5. Then the localisation is performed at the UE by estimating the two AODs and calculating their intersection.

#### *4.3.3.3 Results and outcomes*

A novel architecture is introduced that enables localisation without the need for delay measurements.

#### *4.3.3.4 Perspective and relation to other WP5 contributions*

This architecture is used to perform time resource allocation in a joint localisation and communication system.

### 4.3.4 Contribution #A-3: Receiving RIS to Detect Passive Users

#### *4.3.4.1 Motivation and Context*

The motivation is to use the RIS for environment charting and mapping, and to further detect anomalies and changes in the environment to support active and passive user detection for the purpose of communication, secrecy, and EMF control.

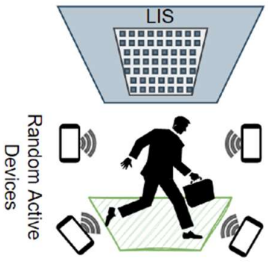


**Figure 4-6 Passive user detection**

#### *4.3.4.2 Methodology*

This method uses a receiving RIS for propagation environment change detection. The method is particularly interesting for the detection of users that do not carry terminals. A brief algorithm description is as follows (see also Figure 4-7):

- The procedure is initiated by the LMF and coordinated by the AMF and RISO.
- A ceiling deployed receiving RIS performs radio sensing (controlled by the RISC) of the transmissions from multiple UES in the near field (spherical wave regime).
- The RIS creates a radio map of the environment as the average field strength over time.
- Change detection between the instantaneous measurement and this map is used to detect new objects in the environment.

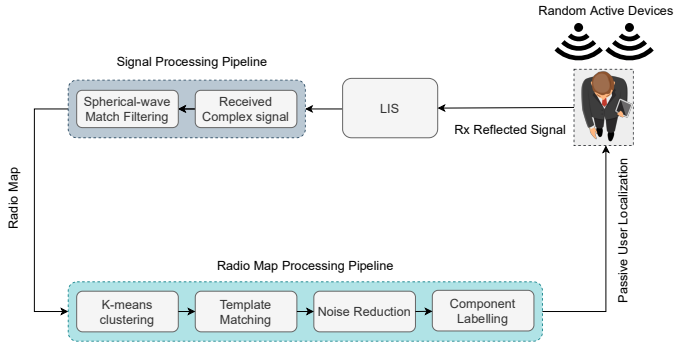


**Figure 4-7. Overview of the methodology for passive user localisation.**

#### 4.3.4.3 Results and Outcome:

The results indicate passive user detection is feasible using sensing and change detection.

#### 4.3.4.4 Perspective and relations to other WPs

This work supports WP4 activities for access, as well as WP6 for EMF aware beamforming.

### 4.3.5 Contribution #A-4 Sensing-RIS-Enabled UE Localisation Without Any Access Points

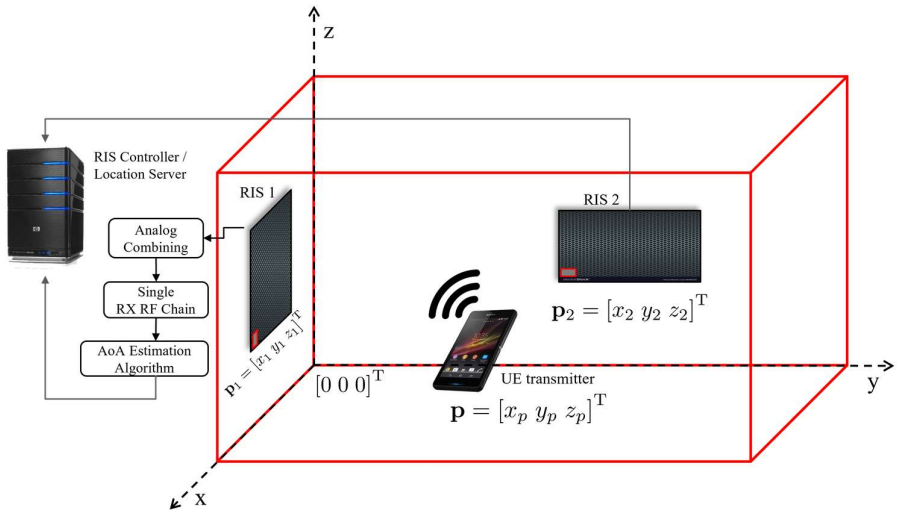


**Figure 4-8. System model of multiple-sensing-RIS localisation without any access points.**

#### 4.3.5.1 Motivation and context

This section introduces a novel localisation sensing-RIS-enabled localisation scenario, without any access points [AVW22]. The architecture consists of one static UE, multiple receiving RISs each equipped with a single Receive (RX) Radio-Frequency (RF) chains attached to all the RIS elements, and one central controller as depicted in Figure 4-8. In an indoor 3D environment with multipath, operating in the mmWave frequencies under the far-field assumption, the localisation AoA estimations for each RIS are being performed and combined at the central controller for the UE to be localized.

#### 4.3.5.2 Methodology

The localisation is performed as follows:

1. The procedure is initiated by the LMF and coordinated by the AMF and RISO.
2. The UE transmits a NB signal.
3. Each RIS receives the impinging signal from the UE with a predefined RIS element configuration (determined by the RISC) and stores it at the central controller.
4. *Step 2.* is repeated each time with a different RIS element configuration (determined by the RISC) until a predefined number of signal measurements are gathered at the central controller, for each RIS.
5. The central controller performs an AoA estimation for each RIS.
6. The central controller fuses the AoA estimations to localise the UE.

#### 4.3.5.3 Results and outcomes

The outcomes of this work are:

- Introducing a localisation scenario with multiple sensing RISs and no BSs.
- Calculating the estimation error for different number of RISs, RISs' placements, and RIS configurations.
- Deriving the CRB for the positioning and comparing with the position estimation error.

#### *4.3.5.4 Perspective and relation to other WP5 contributions*

This section introduced a new sensing-RIS-enabled localisation scenario, which can work in cases with no nearby access points, or act in parallel and supporting transmissions or channel estimation.

### 4.3.6 Contribution #A-5: Mobile RIS Localisation

#### *4.3.6.1 Motivation and context*

This section aims at estimating the 3D location of a user that is equipped with a RIS [KKD+21]. Besides the user, the setup includes one single-antenna BS and *M* single-antenna Rxs, with known positions. Each Rx receives the signal from the BS directly and the reflected signal form the user. Then the localisation is performed based on the collective delay measurements at the Rxs. The system setup is illustrated at Figure 4-8 (separation of different users will be discussed in Section 5.2.2). This setup has two benefits in terms of localisation: first, using only delay measurements enables simplification of the estimation method, and second, in this setup the users do not receive or transmit any signals and only use a single RIS, which makes this setup ideal for localizing passive objects.

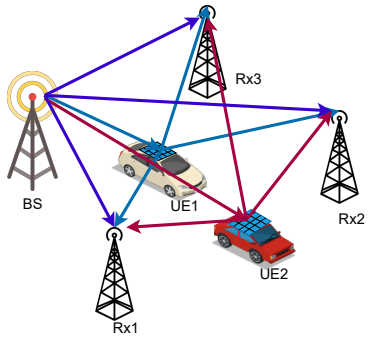


**Figure 4-8: System setup for RIS-enabled passive localisation with 2 UEs and 3 Rxs.**

#### *4.3.6.2 Methodology*

The localisation consists of two steps, is initiated by the LMF and coordinated by the AMF and RISO:

1. Calculating the propagation delay at each Rx and associating them to their corresponding path
2. Using the delay measurements to estimate the users' position

To perform the first step, an orthogonal RIS phase profile is designed based on the elements of the FFT matrix of size *N+1*. The profiles between different RISs are determined by the RISO. The RISs are controlled by their local RISC. Then a pre-processing step is performed at each Rx to separate the *N+1* signal paths from each other. By doing so, the delay of each path can be readily calculated via standard methods based on the FFT transform. After calculating the delays, the user position is estimated based on geometrical relations, which results in calculating the intersection of *M* ellipsoids in 3D.

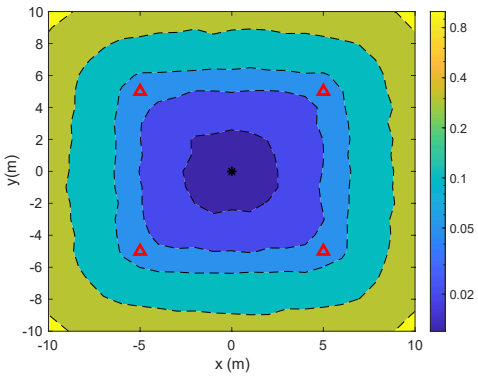

**Figure 4-9: PEB in meters for four RXs (shown by red triangles) and one user. The BS is shown by a star.**

#### *4.3.6.3 Results and outcomes*

The main outcomes of this section are

- Developing a low-complexity estimator for localizing multiple passive users based on the delay measurements.
- Developing theoretical bounds that provide a lower bound on the estimation error.
- In Figure 4-9, the PEB in meter is shown for a system with 1 BS at height *4*m, *4* Rxs at height *3*m and the user at *0*m.

#### *4.3.6.4 Perspective and relation to other WP5 contributions*

Localisation of a mobile RIS is considered, which could be used to calibrate RIS locations in other WP5 contributions.

# 5 RIS control methods

## 5.1 Localisation and sensing perspective

The practical accuracy achievable within RIS-assisted localisation is strongly bounded to the chosen RIS control strategy. There are several inter-related aspects to this:

1. Acquiring the necessary channel state information (CSI) to determine optimized RIS configurations.
2. Optimisation and dynamic control of RIS configuration (i.e., controlling the complex coefficients and/or only the phases of the RIS unit cells), optimised for localisation or sensing performance.
3. Accounting for real RIS hardware limitations in the above two steps.

### 5.1.1 CSI acquisition

For data communication purposes, this problem can be solved through the estimation of cascaded channel responses by using successive pilots and varying the RIS configurations between pilot transmissions. Then the cascaded channel can be recovered by least-squares estimation [SZL+21]. However, in case of RIS-based localisation, this approach might be suboptimal depending on the specific localisation scenario (e.g., DL/UL transmissions, 2D/3D, estimated radio metrics available as observations, near-field/far-field regime, targeted state variables). For instance, simpler random RIS phase profiles could enable asynchronous positioning in downlink single-input- single-output (SISO) multi-carrier (MC) transmission contexts, while many successive transmissions are needed. This scheme does not require any prior information (neither about the channel, nor about the UE location), but is not optimal under a priori UE location information.

### 5.1.2 RIS optimisation

For data communication, concentrating power towards the user to be served and accordingly, concentrating signal-to-interference-and-noise-ratio (SINR), is a meaningful approach to optimise communication rate. For localisation and sensing, RIS profiles can be configured to optimize the static PEB (and/or the orientation error bound (OEB)), even in more generic multiple inputs multiple outputs (MIMO) MC contexts, based on the prior UE location. In this case however, the actual uncertainty regarding this prior knowledge in a real system (typically, while using the latest known location estimate instead of the perfect knowledge, along with its covariance) can be incorporated by design in the optimisation problem.

### 5.1.3 RIS hardware limitations

Finally, real RIS hardware limitations shall be considered in the control design too. In general, there exist several theoretical models for phase control, quantized phase control, amplitude-dependent phase control, and joint amplitude and phase control, which all require tailored optimisation. Another unified way of treating these models consists in relying on lookup tables instead, which list all realizable amplitudes and

phases in practice at each element with a given RIS hardware. Such tables can also account for coupling effects, which are challenging to treat analytically. All in all, the optimisation of RIS configuration (based on real lookup tables or more conventional model-based descriptions) could hence be performed prior to or after constraining the problem by real hardware capabilities, potentially with a strong impact onto performance (e.g., in terms of beam peak power, achievable beam shape, secondary lobes).

## 5.2 Contributions from RISE-6G

An overview of the different contributions is provided in Table 5-1.

**Table 5-1. Overview of the RIS control contributions.**

| Control parameter | Con. C-1: Joint BS and RIS Precoding for Localisation | Con. C-2: Profile Design for Multiple RIS Orthogonalizations | Con C-3 Localisation with Directional and a Random Codebook without BS | Con. C-4 RIS Phase Design under User Mobility and Spatial Wideband Effects | Con. C-5: RIS profile control for non-line-of-sight conditions | Con. 6: RIS profile control under realistic implementation |
|---|---|---|---|---|---|---|
| Purpose (optimisation criterion) | Positioning performance (PEB) | Orthogonality among different RIS | Positioning performance | Positioning performance | Positioning performance | Positioning performance |
| What is optimized (variables) | RIS and BS profile jointly, BS power allocation | RIS profiles across several RIS | RIS phase profiles | RIS phase profile | RIS phase profile | RIS phase profile |
| Quantisation | No | No | No | No | No | Yes |
| RIS element model (incl. quantisation) | Phase | Phase | Phase | Phase | Phase | Phase with coupled amplitude |
| Codebook | Directional and far-field derivative beams | Random | Directional and random | Direction and random | Directional and near-field derivative beams | Lookup-table |
| Number of configurations | Several (depends on uncertainty range) | Several (depends on integrated SNR requirement and number of RIS) | Several are needed | Several are needed | Several are needed (4 distinct) | Several are needed (4 distinct) |
| Architecture and RIS knowledge | Same as Contribution #A-0. Passive static RIS, known position and orientation. | Same as Contribution #A-0. Passive mobile, unknown position, and orientation. | Same as Contribution #A-1. RIS with known position and orientation. | Same as Contribution #A-0. Passive static RIS, known position and orientation | Same as Contribution #A-0. Passive static RIS, known position and orientation | Same as Contribution #A-0. Passive static RIS, known position and orientation |

### 5.2.1 Contribution #C-1: Joint BS and RIS Precoding for Localisation

#### *5.2.1.1 Motivation and context*

The aim of this section is to study the problem of RIS-aided joint localisation and synchronisation of a single-antenna UE using downlink signals transmitted by a multiple-antenna BS (i.e., MISO scenario) [FKC+21]. To optimize the localisation and synchronisation performance in this scenario, which is depicted in Figure 5-1, a joint design of active transmit precoding at the BS and passive phase profiles at the RIS is considered. The jointly optimized design exploits the a-priori information on UE location and

avoids high computational burden by resorting to a codebook-based approach. In addition, a low-complexity ML estimator of UE location and clock bias is developed and shown to achieve the theoretical bounds even at low SNRs and in the presence of uncontrollable multipath components. The mean benefit associated with the use of a single-antenna UE is that it can be particularly attractive for 6G networks with a high amount of low-power, low-cost devices.

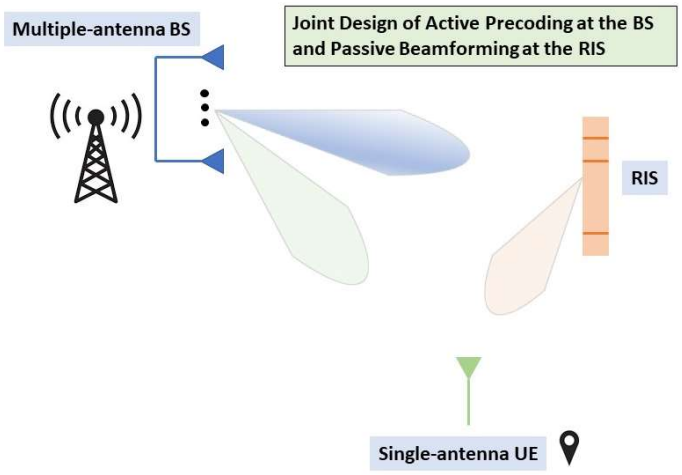


**Figure 5-1: Illustration of the scenario for RIS-aided downlink joint localisation and synchronisation of a single-antenna UE. To maximize the localisation accuracy of the UE, active precoding at the BS and passive RIS phase profiles can be jointly designed by resorting to a codebook-based strategy that employs both conventional directional beams and novel derivative beams.**

#### *5.2.1.2 Methodology*

Our methodology to tackle the problem of RIS-aided joint localisation and synchronisation is as follows:

- First, theoretical bounds on UE location (PEB) and clock bias (CEB) estimation are derived, leading to performance metrics that can be used to design BS precoder and RIS phase configurations.
- The next step is to formulate the joint design problem and explore the convexity properties with respect to the optimisation variables (i.e., BS and RIS beams). Based on the structure of the problem, the optimal beam sequences at the BS and RIS can be determined.
- Under imperfect knowledge of UE location, a novel codebook-based design is provided, with an optimized power allocation of codebook entries at the BS side.
- A reduced-complexity ML estimator, called the joint maximum likelihood (JML) estimator, is derived to estimate location and clock offset.
- Extensive simulations are performed to showcase the performance improvements via joint design of BS precoders and RIS profiles in both theoretical bounds and RMSEs achieved by the proposed estimator.

#### *5.2.1.3 Results and outcomes*

Several benchmark schemes are considered to compare the performance of the proposed designs.

- Directional Codebook (uniform power allocation): conventional *directional* beams with equal powers, that cover the uncertainty region of the UE.
- Directional Codebook (optimized power allocation): conventional *directional* beams with power allocations optimized to minimize the PEB and/or CEB.
- DFT Codebook (optimized power allocation): DFT beams corresponding to the columns of the DFT matrix, where beam powers are optimized to minimize the PEB and/or CEB.

- Proposed Codebook (optimized power allocation): *directional* and *derivative* beams (see Figure 5-2) with optimized powers, spanning the uncertainty region of the UE.

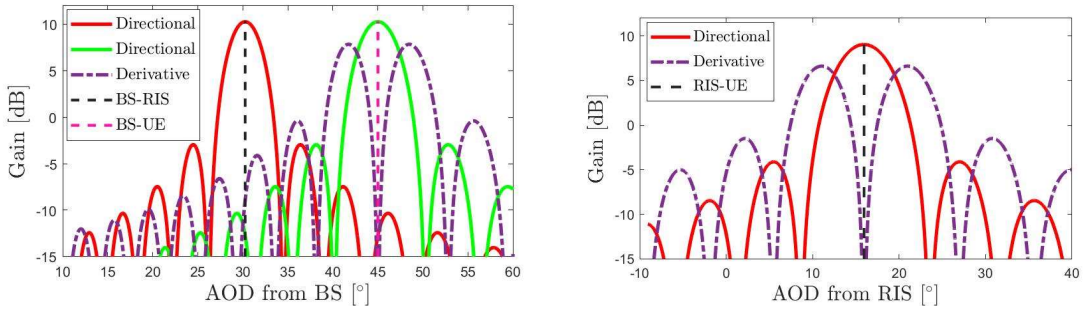


**Figure 5-2: Beampatterns of the proposed localisation-optimal BS and RIS beams consisting of both directional and derivative beams. Directional beams maximize SNR at the desired location, while derivative beams allow the UE to optimally identify small deviations around the nominal direction, which improves AoD and localisation performance.**

In Figure 5-3, RMSEs on the UE location and clock offset estimation, obtained by the proposed JML estimator using the considered codebook designs, are presented. As can be noticed, the proposed codebook provides noticeable accuracy gains in both localisation and synchronisation. In addition, to evaluate the robustness of the proposed estimator against uncontrollable multipath propagation, the localisation RMSEs in both the presence and absence of uncontrollable paths are presented in Figure 5-4. It is seen that the JML estimator is highly robust, especially at high SNRs.

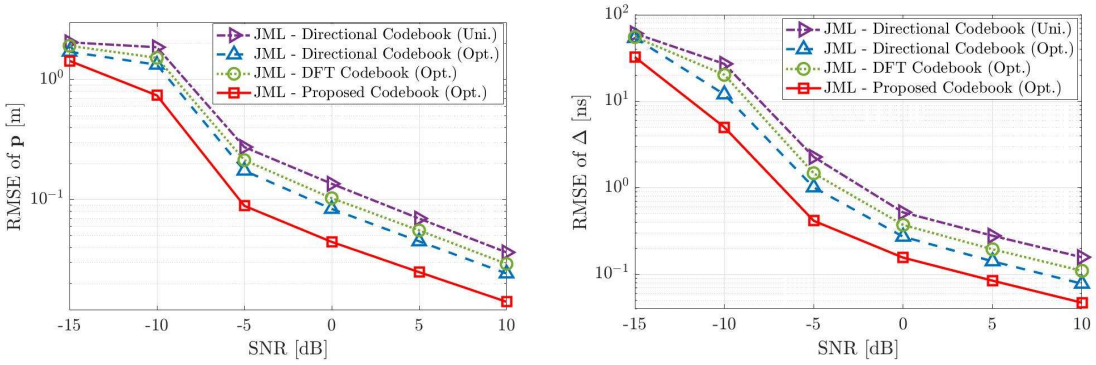


**Figure 5-3: RMSE of location and clock offset estimation, obtained by the proposed joint maximum likelihood (JML) estimator using the benchmark and the proposed BS-RIS codebooks.**

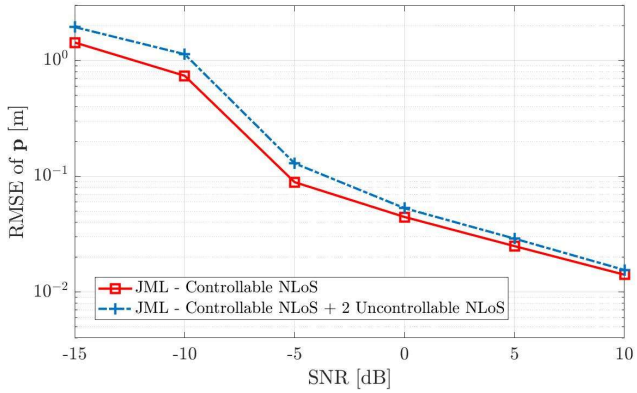


**Figure 5-4: Localisation performance of the JML estimator with respect to SNR with and without uncontrollable NLOS propagation.**

The main outcomes of this study are as follows:

- Joint design of localisation-optimal BS precoders and RIS phase profiles, considering practical constraints such as unit-amplitude RIS weights and UE location uncertainty.
- Development of a low-complexity location and clock offset estimator.
- Illustration of performance improvements using proposed BS-RIS signal design, with and without uncontrollable multipath propagation.

#### *5.2.1.4 Perspective and relation to other WP5 contributions*

The analysis and designs for the RIS-aided MISO localisation scenario in this section complements the RIS phase profile designs for the RIS-enabled SISO scenarios and provides a unified treatment on location/clock offset estimation and beamforming design for single-antenna devices.

### 5.2.2 Contribution #C-2: Profile Design for Multiple RIS Orthogonalizations

#### *5.2.2.1 Motivation and context*

This section aims at estimating the 3D location of $N$ users that are equipped with RISs, which has been studied in the contribution [KKD+21]. It deals with the separation of users in the contribution from Section 4.3.6. The main challenge here is to perform data association, i.e., to assign different delay measurements to their corresponding paths at each Rx. To overcome this challenge a temporal orthogonal RIS phase design can be used. This approach is like the one used in the RFID literature [NZS11], [QPZ17]. In [YDW+21], each RIS modulates the impinging wave with its own frequency shift, by which the destination can recognize it.

#### *5.2.2.2 Methodology*

The temporal orthogonal RIS phases can be used to avoid interference between multiple paths reflected from RISs and solves the data association problem. Here, a high-level explanation of this method is provided. For more information, please see the paper [KKD+21]

1. Each of the UEs select a fixed RIS phase profile (it can be random or directional or include any arbitrary phases)
2. At each time, each UE multiplies its selected phase profile by a scalar that may be different from other UEs
3. The series of scalars over time are selected such that they constitute orthogonal codes between the users
4. Since the channel is linear, the received signals from each of the UEs is also multiplied by the same scaler. Therefore, at the end of the transmission each of the receivers can use the orthogonal codes to distinguish the signal received from different users

#### *5.2.2.3 Outcome*

The main outcomes are the presentation a generic method to separate different signal paths that reflects from different RISs at the Rx. This method uses RIS phase profiles that are orthogonal in time.

#### *5.2.2.4 Perspective and relation to other WP5 contributions*

The outcome of this section can be used in any area that benefits from separating different paths arriving from different RISs at the Rx. Specifically, the results that are based on single-RIS localisation (such as MISO and SISO localisation) can be extended to multi-RIS systems.

### 5.2.3 Contribution #C-3: Localisation with Directional and a Random Codebook without BS

#### *5.2.3.1 Motivation and context*

This section compares the localisation accuracy for a directional and a random phase profile for the setting where the UE is localised with one RIS without any BSs described in [KSA+22], as previously described in Figure 4-3. With the random codebook, all the phase shifts for the RIS elements are set randomly. With the directional one, it is assumed that there exists a prior knowledge on the UE location. Specifically, that the user is located within a sphere. Then RIS phase profile is generated by directing the signal to multiple points that are selected randomly within this sphere. It is shown that with the directional phase profile the estimation error is approximately one order of magnitude less than the estimation error with the random codebook.

#### *5.2.3.2 Methodology*

To perform localisation:

- The user transmits a wideband signal
- The RIS applies phase shifts based on a codebook to the signal and reflects it back to the user. The RIS can use directional codebook (if a prior information on user location is available) or random one.
- The user processes the reflected signal and calculates the user location by optimizing the log-likelihood function.

#### *5.2.3.3 Results and outcomes*

To compare the directional and random phase profiles, the CRB bounds, and the estimation error is evaluated for different user positions and different RIS sizes. Figure 5-5 compares the PEB in for directional and random codebooks at the user position p=[10,10,10] meters. It is shown that with a higher number of RIS elements, the gap between the CRBs of the directional and random codebook becomes larger. This is since with directional beamforming the SNR increases quadratically with the number of RIS elements, while it grows linearly in case of random codebook. Also, with low number of RIS elements, the PEB is worse for directional codebook because, due to the large beamwidth, the transmitted beams will be almost identical and the FIM becomes ill-conditioned for the lack of beam diversity. However, for larger (and more standard) number of RIS elements, the directional codebook obtains a better PEB.

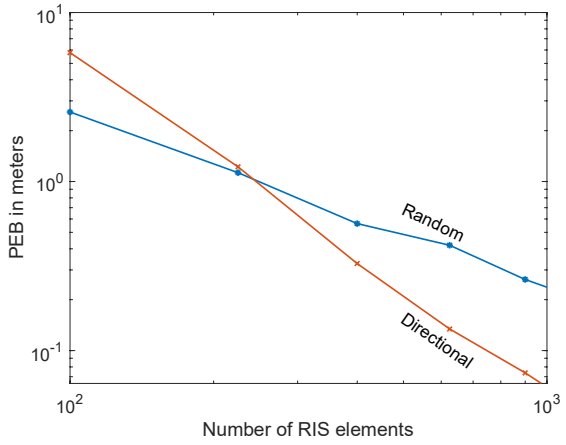


**Figure 5-5: comparing random and directional codebooks in terms of PEB for different numbers of RIS elements at the point *p=[10,10,10]* meters.**

#### *5.2.3.4 Perspective and relation to other WP5 contributions*

Other codebooks such as the one that minimizes the PEB as in [KJM+22] can be used and the results can be compared to the two codebooks considered here.

### 5.2.4 Contribution #C-4: RIS Phase Design under User Mobility and Spatial Wideband Effects

#### *5.2.4.1 Motivation and context*

This section considers user localisation in a SISO system with an RIS as shown in Figure 4-2. The localisation is performed by measuring the delay for the direct and indirect paths and the AOD from the RIS to the user. The channel model is developed by considering the user mobility and the spatial wideband effects. The user mobility has been considered in a number of works that studied RIS aided communication [MBD+21][Bas19] , but this effect in the localisation literature is under studied. Similarly, the spatial wideband effects, have been studied for MIMO [WGJ+18][CGN+16] and RIS-aided communication systems [DAN+21][MSA+21], but not for RIS-aided localisation framework. Two different RIS phase profiles are considered: random codebook and directional codebook. With the directional codebook it is assumed that a prior knowledge about the user position is available. To separate the direct and indirect paths from each other, temporal orthogonal phase profiles and a post processing step is performed. A low-complexity estimator is developed to estimate the user position, clock bias and velocity. The estimator considers the user movement but not the spatial wideband effects.

#### *5.2.4.2 Methodology*

To perform localisation, first the delay and the velocity of the direct path is calculated and then the direct path is subtracted from the received signal. Then the estimator calculates the AOD, delay and the radial velocity of the indirect path. To counter the effects of user mobility the Doppler effects are compensated for in an iterative fashion. Finally, the user position is estimated based on the AOD (which represents a line in space) and the TDOA between the direct and indirect path (which represents a hyperboloid). Also, the CRB lower bounds are calculated as benchmarks.

#### *5.2.4.3 Results and outcomes*

The localisation performance is measured by CRBs as well as the estimation error. The following results are obtained:

- A RIS channel model is developed that considers user movement and the spatial wideband effects.
- A low-complexity estimator is developed and CRB bounds are calculated. It is shown that the estimation error is close to the CRBs when the wideband effects are small (with small RIS or small bandwidth).

- The localisation performance is compared between directional and random codebooks, and it is shown that the directional codebook outperforms the random one by an order of magnitude. Furthermore, it is shown that wideband effects are more pronounce in directional codebook than the random one.
- Figure 5-6shows the PEB and the estimation error for random and directional codebooks. The estimation error is very close to the theoretical bounds. The effects of spatial wideband effects can be seen for directional codebooks and for frequencies more than 400 MHz. In this regime, the error of the estimator, which is designed based on the narrowband model, becomes noticeably larger than the PEB due to the spatial wideband effects.

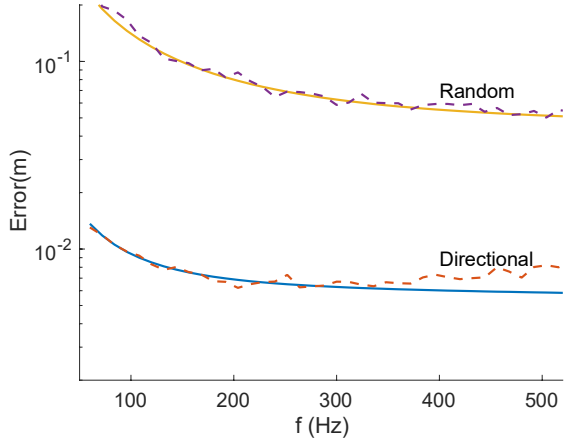


**Figure 5-6: PEBs (solid lines) and estimation errors (dashed lines) in presence of spatial wideband effects vs signal bandwidths. Random and directional codebooks are considered. The RIS size is 32 x 32.**

#### *5.2.4.4 Perspective and relation to other WP5 contributions*

Other localisation contributions can be extended by considering the wideband effects and the user mobility as is done in this section.

### 5.2.5 Contribution #C-5: RIS profile control for non-line-of-sight conditions

#### *5.2.5.1 Motivation and context*

As already raised here, one important challenge in the context of RIS-aided wireless localisation consists in optimizing the RIS profiles, especially when operating in the reflective mode (i.e., optimizing their reflection coefficients and/or their phase profiles in case of uncontrolled reflection amplitude). While conventional solutions intended for RIS-aided communications mostly aim at increasing SINR at the UE based on the estimation of cascade channels or on prior UE location information (e.g., [ADD21], [HZZ+20]), more specific RIS beam patterns must hence be designed (from a RIS precoding standpoint), according to the overall localisation strategy considered at the system level (incl. the extracted location-dependent metrics, the transmission settings, or the availability of prior information…). This problem is particularly critical in case of NLoS propagation, where RIS-reflected paths are needed to compensate for the loss of the direct path and enable localisation accordingly (incl. within single-RIS settings in near-field). Relying on prior works on far-field (FF) LoS localisation over downlink (DL) single-input-single-output (SISO) multicarrier (MC) transmissions using a reflective RIS [KKS+21b], as well as on near field (NF) localisation with a receiving RIS [GD21], [AKK+21], this contribution aims at designing new localisation-optimal phase profiles for reflective RISs (i.e., precoding schemes) that contribute to minimizing DL positioning performance bounds (used as optimisation cost) in NLoS conditions.

In terms of system architecture and signalling, a basic SISO DL positioning scenario is considered here, with 1 single-antenna BS, 1 single-antenna UE, 1 planar RIS in reflective mode assuming a variable number of elements (See Figure 5-7), and a generic transmission model encompassing both NF and FF regimes, as well as the transmission of multiple DL pilot signals. Accordingly, the UE is in charge of

estimating the relevant location-dependent radio metrics out of received signals, while the final computation of the estimated position can be performed either on the UE's side or in a distant centralized server, provided that the measured radio metrics are transmitted from the former.

As for the system setup, it is assumed a 3D localisation case (even though, for simplification, performance is assessed in a pseudo-2D plane), a mmWave operating frequency (typically at 28GHz) benefiting from the geometric nature of the channel, although most of the provided developments are agnostic w.r.t. frequency. Both NF and FF propagation regimes are also considered, as well as both LoS and NLoS components, although the performance is assessed mainly in the presence of blockage, where the RIS's added value is the most obvious w.r.t. localisation continuity. No rich scattering or extra-interferences resulting from « natural » multipath (i.e., besides the resolvable direct and RIS-reflected paths) have been considered so far.

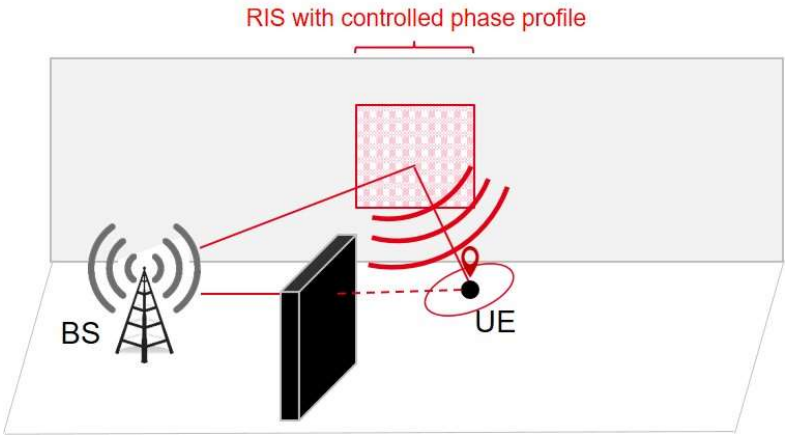


**Figure 5-7. Canonical scenario considering optimising reflective RIS profiles in NLOS SISO DL positioning.**

#### *5.2.5.2 Methodology*

The potential of a single reflective RIS to combat NLoS effects in geometric NF conditions is first investigated in terms of localisation feasibility and continuity, while assuming non-optimized (i.e., random) RIS profiles. The first step of this contribution can be summarized as follows [RDK+21]:

- Based on a generic RIS response model accounting for both NF and FF regimes, a DL SISO MC localisation problem is stated in both LoS and NLoS propagation scenarios.
- Accordingly, a Fisher information analysis is performed, characterizing the fundamental bounds on positioning performance (from channel parameters Fisher Information Matrix (FIM) to positional FIM in Cartesian coordinates), including identifiability considerations. The latter makes it possible to conduct a sensitivity study of the Position Error Bound (PEB) w.r.t. key system parameters, such as the number of RIS elements, the operating frequency, or the number of consecutive symbols transmitted by the BS, the UE distance to the RIS and more, all while assuming random RIS profiles.

Then, leveraging on the previous theoretical bound calculation from [RDK+21], the design of more suitable phase profiles is proposed for a reflective RIS through PEB optimisation to further enhance positioning accuracy in the NLoS context [RDK+22a]. This second step of the contribution is hence summarized as follows:

- The closed-form expressions of both the positional FIM (in both Spherical and Carte-sian coordinates) and the resulting PEB in the DL SISO SC context are derived, while assuming a generic NF-compliant formulation for the RIS response.

- A PEB optimisation problem is stated, assuming the prior knowledge of UE position and after a few mathematical manipulations, a low-complexity method is proposed to solve the problem and retrieve the corresponding localisation-optimal RIS phase profiles accordingly.
- The performance of the resulting localisation-optimal phase profiles is compared with that of conventional random [RDK+21] and directional [AKK+21] designs, in terms of achievable PEB.
- Finally, both the shapes and the relative weights of the RIS beam and its successive derivatives (w.r.t. each spherical coordinate), as involved in the localisation-opti-mal solution, are illustrated and discussed.

#### *5.2.5.3 Results and outcomes*

First simulation results in a canonical SISO DL MC scenario with random RIS profiles [RDK+21] confirm the benefits from a single-RIS reflection in NF to enable localisation continuity (See Figure 5-8 and Figure 5-9). Accordingly, whenever the UE is close enough to the RIS and/or when the RIS is large enough, exploiting the signal wavefront curvature of the reflected multipath component in NF could be sufficient to directly infer user's position in the absence of direct path, even if the achievable NLoS accuracy is shown to be relatively low.

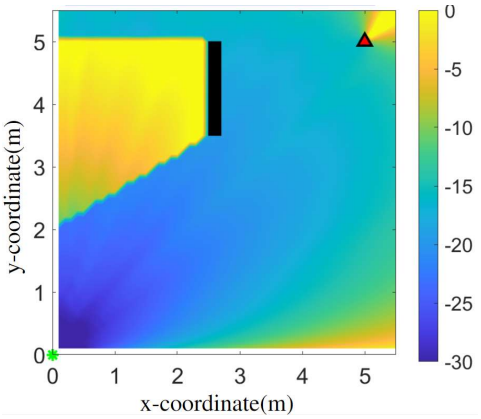


**Figure 5-8. PEB heatmap (in dB), as a function of UE location (z = 0) for a generic RIS response model (supporting NF), with one planar reflective RIS of 32x32 elements in [0, 0, 0]m, one BS in [5, 5, 0]m and a finite obstacle parallel to the y axis (black).**

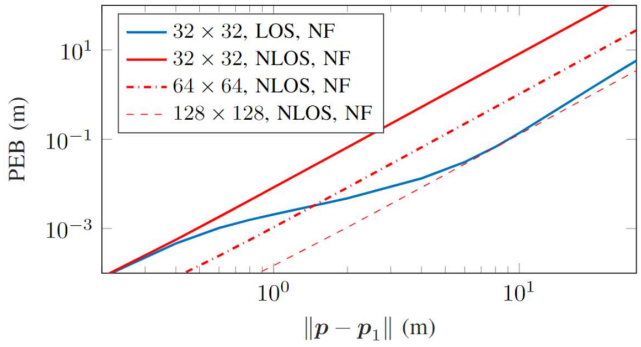


**Figure 5-9. PEB (in m) as a function of the UE-RIS distance with one RIS of 32x32, 64x64 and 128x128 elements in**

Overcoming this problem of limited NLoS positioning accuracy, other numerical simulations in a canonical SISO DL SC scenario [RDK+22] show that the proposed localisation-optimal RIS profile clearly outperforms conventional random and directional beam codebook designs in terms of PEB (See Figure 5-11 below). It is also shown that the theoretical optimal solution would involve a weighted combination

of four beams at the RIS (i.e., one directional beam, along with its derivatives w.r.t. space dimensions), whose respective weights can be determined through the PEB minimisation procedure (See Figure 5-10 below).

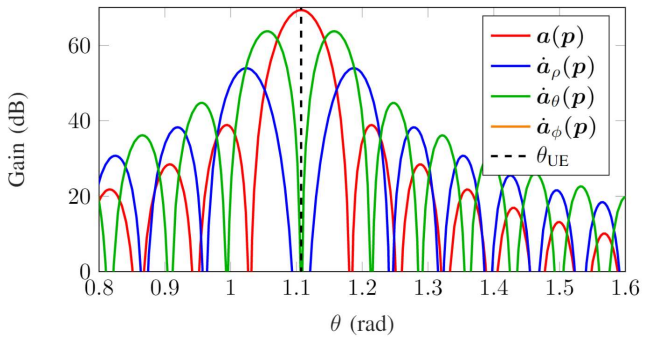


**Figure 5-10. Illustration of localisation-optimal orthonormalized beams to be theoretically applied at the reflective RIS (i.e., incl. directional beam in red, along with its 3 derivates w.r.t. spherical coordinates, resp. in blue, green, and orange), as a function**

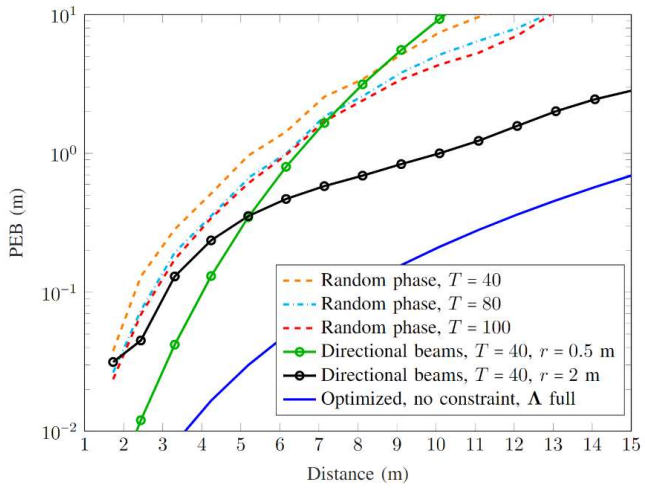


**Figure 5-11. PEB comparison as a function for the UE-RIS distance, with the proposed optimized RIS profile, conventional directional and random codebook designs, for a different number of transmissions T and different prior UE position uncertainty (for directional b**

This contribution is subject to one paper publication [RDK+21] and one paper submission [RDK+22a], whose full-extent preprint versions are accounted in the Appendices.

#### *5.2.5.4 Perspective and relation to other WP5 contributions*

Related works concern the adaptation of the previous optimisation scheme to more realistic implementation and/or hardware contexts (i.e., constraining the « feasible » beams), as summarized in 5.2.6. Future works regard the extension of the previous control schemes into dynamic scenarios, combining RIS control with dedicated positioning and tracking estimators while re-injecting the latest position estimate, with its presumed uncertainty, as prior knowledge into the RIS profile optimisation stage.

### 5.2.6 Contribution #C-6: RIS profile control under realistic implementation

#### *5.2.6.1 Motivation and context*

After determining the optimal complex profiles of reflective RISs for NLoS DL positioning in NF through unconstrained PEB optimisation (See Section 5.2.5), related implement-ability issues are also addressed

in this subsection. RISs are usually made of low-cost hardware and may suffer more from imperfections than a standard infrastructure [HRE18], [SXG+20]. The « feasible » beams to be generated at the RISs are a priori strongly constrained practice or at least they are bounded to look-up tables characterizing the element-wise reflection coefficients of real hardware RISs.

One first motivation for this contribution is hence to propose and benchmark several sub-optimal implementation variants of the initial PEB optimisation scheme that could offer different trade-offs in terms of practicability, complexity, and performance.

Another goal is to offer a practical optimisation framework capable of approximating any desired beam pattern directly from lookup tables (typically, the directional and derivative beam patterns required to optimize NLoS DL positioning in NF), given a real RIS hardware, i.e., two reflect-arrays developed and characterized in the frame of RISE-6G WP3.

In terms of both architectures, signalling and system setup, the same configuration as that of Section 5.2.5 is considered here, although the contribution related to lookup tables is somehow more general and agnostic.

#### *5.2.6.2 Methodology*

First, practical sub-optimal algorithmic solutions are compared, which can retrieve « feasible » RIS phase profiles through PEB optimisation, while considering the profiles to lie on the unit circle [RDK+22a]:

- In one variant, referred to as *Optimize then constrain* scheme, an optimisation with unconstrained profiles is first performed, before constraining the resulting solution by applying a gradient projections method [TSF+17]
- In a second variant, referred to as *Constrain then optimize* scheme, the RIS profiles is first constrained a priori following a similar gradient projection approach and then these projections are injected as an input into the optimisation problem
- For any of the two previous variants, an equivalent time-sharing implementation is proposed, which allocates a certain amount of time (i.e., a certain number of successive DL symbols) to each of the required « feasible » profiles that must be sequentially applied at the RIS, according to their optimized relative weights.
- The PEB performance of these suboptimal algorithmic variants is compared with both that of the localisation-optimal (unconstrained) solution, as well as that of conventional random and directional designs

Then, a computationally efficient and low-complexity method is introduced to optimize the configurations of reflective RISs from an arbitrary lookup table (including RIS element responses based on real measurements), to approximate arbitrary complex beam patterns [RDK+22b]:

- More specifically, the proposed approach also first applies the projected gradient descent algorithm as previously [TSF+17] to constrain the RIS profile w.r.t. the look-up table. Then, the complex beam pattern is expressed in terms of spherical coordinates and the objective function aiming at matching the synthesized beam with the desired one is re-defined to enable precise approximation only for a subset of reference points in the overall 3D domain, hence drastically reducing complexity.
- The proposed approach is illustrated for several beam types, including that required to optimize the NLoS DL positioning performance (i.e., directional beam and its derivatives) for several real lookup tables with measured elementwise RIS reflection coefficients consisting of quantized phases and realistic amplitude losses.

#### *5.2.6.3 Results and outcomes*

Regarding the constrained unit-modulus RIS profiles, simulations [RDK+22a] show that the *Constrain then optimize* scheme significantly outperforms the *Optimize then constrain* scheme, while being close to the performance of the optimal scheme with unconstrained RIS profiles Figure 5-12. Also shown is that the time-sharing scheme, assuming the application of each feasible beam sequentially enables us to approach the performance of the PEB-optimal solution, with very limited performance degradation when the overall number of DL transmissions is sufficiently large (See Figure 5-13).

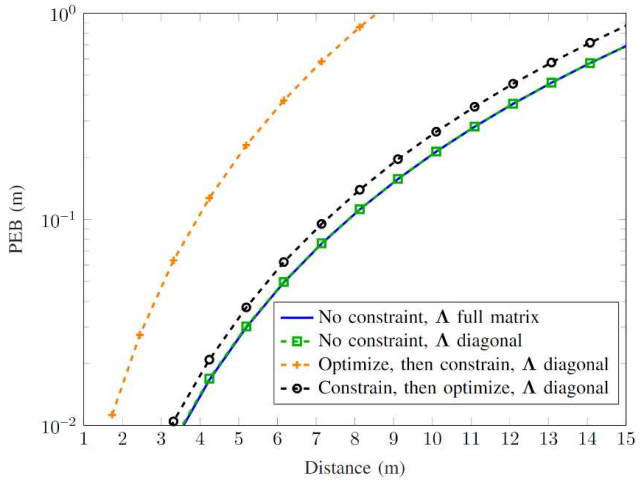


**Figure 5-12. PEB as a function of the distance for different variants of the problem solver (incl. the unconstrained/optimal, *Optimize then constrain* and *Constrain then optimize* schemes).**

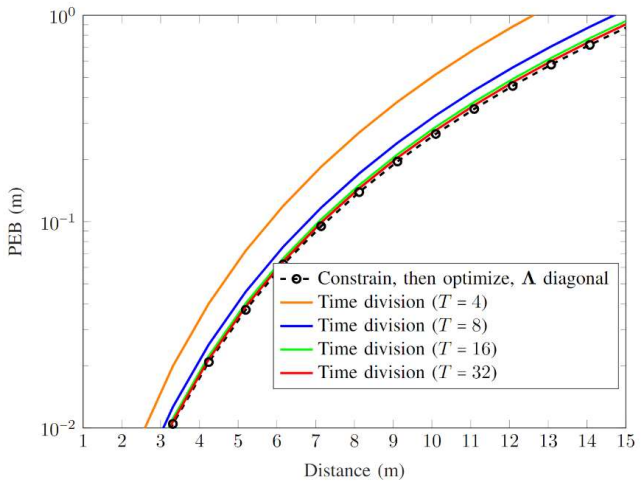


**Figure 5-13. PEB as a function of the RIS-UE distance with both the Constrain then optimize scheme and its practical implementation through time-sharing depending on the total number of DL transmissions T.**

Another set of simulations [RDK+22b] stresses out the dominating impact of both phase quantisation levels and the span of practically valid phases, as well as power loss, of the element-wise reflection coefficients within real RIS hardware, w.r.t. the beam peak power generated in the desired RX direction(s) (Figure 5-14) and to the presence of harmful undesired lobes (Figure 5-15).

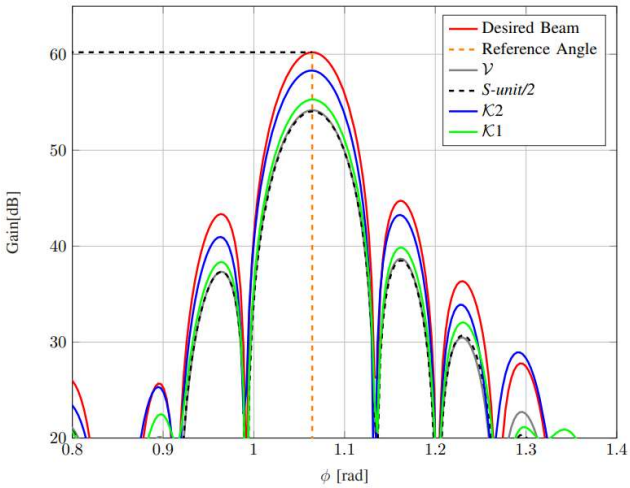


**Figure 5-14. Directional beam patterns as a function of the elevation angle for various beam synthesis methods under gradual RIS hardware constraints, including the RIS element responses from real hardware developed in RISE-6G WP3.**

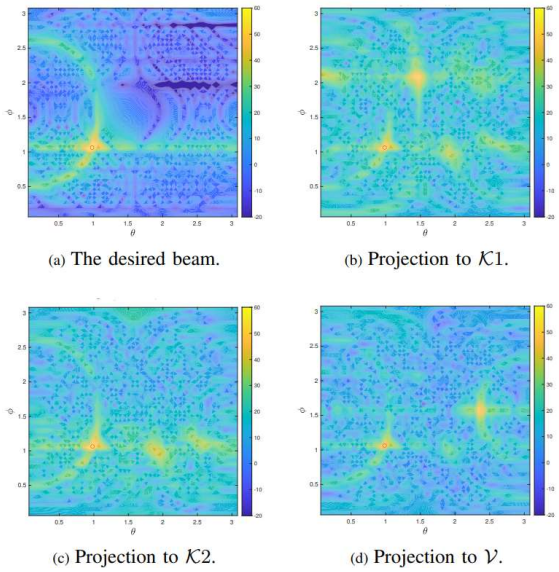

(a) The desired beam. (b) Projection to $\mathcal{K}1$.

(c) Projection to $\mathcal{K}2$. (d) Projection to $\mathcal{V}$.

**Figure 5-15. Illustration of a directional beam pattern pointing to one single desired direction (red circle), as a function of elevation and azimuth angles (desired beam vs. beams synthesized under lookup table characterisation from real hardware (e.g., with RIS e**

This contribution has been subject to one paper publication [RDK+22a] and one paper submission [RDK+22b], whose full-extent preprint versions are accounted for in Appendices.

#### *5.2.6.4 Perspective and relation to other WP5 contributions*

Future works should investigate more extensively and quantitatively the practical performance of RIS-aided positioning and sensing at the system level with the proposed low-complexity algorithmic methods while considering the latest updates from WP3 in terms of both hardware characterisation (i.e., lookup tables from new upgraded hardware) and RIS models.

# 6 Data flow and signalling

In this section, the data flow and signalling, as well as the time diagrams of the RISE-6G architectures from the individual contributions from Section 4 and Section 5, are provided. The summary can be found in Table 6-1. Note that in many of the alternatives, the amount of control information sent to the RIS (more explicitly, each RISC) depends on the local autonomy of the local RISC. For instance, if the RIS is to generate directional beams towards a UE, the control information could be the position of the UE (in which case the RISC computes which beams to generate) or a sequence of RIS configurations (in which case the RISC simply activates each of these configurations sequentially).

**Table 6-1. Alternatives for data from and signalling, related to the RISE-6G contributions.**

| Data flow and signalling alternative | Related RISE-6G contributions from Section 4 | Related RISE-6G contributions from Section 5 |
|---|---|---|
| Alternative 1: UE localisation from a single BS, aided by a reflecting RIS | A-0, A-2 | C-1, C-4, C-5, C-6 |
| Alternative 2: User localisation without access points | A-1 | C-3, C-6 |
| Alternative 3: UE Localisation with multiple sensing RISs, without any BS | A-4, A-3 | C-3, C-6 |
| Alternative 4: Semi-passive localisation of RIS-enabled users | A-5 | C-2 |

## 6.1 Alternative 1: UE localisation from a single BS, aided by a reflecting RIS

Data and control flow of Contribution A-0 is shown in Figure 6-1, and the corresponding time diagram is in Figure 6-2. The diagrams are also applicable to Contribution A-2, by extending to several RIS, operating in parallel. The diagrams are also applicable to Contributions C-1, C-5, C-4, and the first part of contribution C-6 where the second part, which deals with beam approximation using RIS, is agnostic to such schemes. In some cases, the RIS configurations depend on the current knowledge of the UE position.

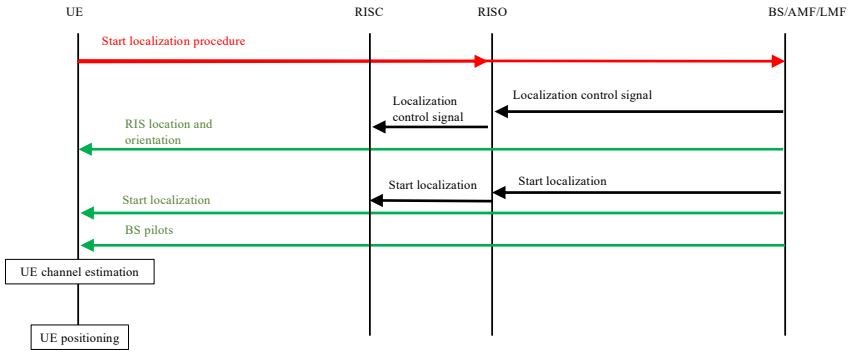


**Figure 6-1. Data and control flow Alternative 1. Note that the position estimation does not need to be performed at the UE side, and that the flow can also be done in UL.**

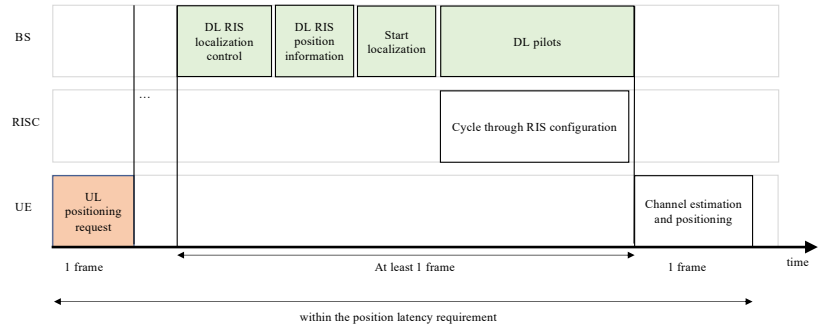


**Figure 6-2. Time diagram Alternative 1.**

## 6.2 Alternative 2: User localisation without access points

Data and control flow of the Contributions A-1 and C-3 is shown in Figure 6-3, where the UE communicates the control signals either with a BS or directly with the RIS control unit. The corresponding time diagram is presented in Figure 6-4.

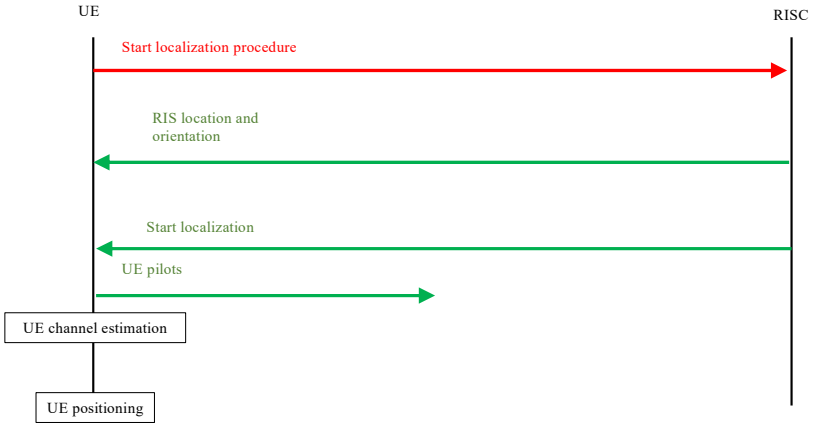


**Figure 6-3. Data and control flow Alternative 2.**

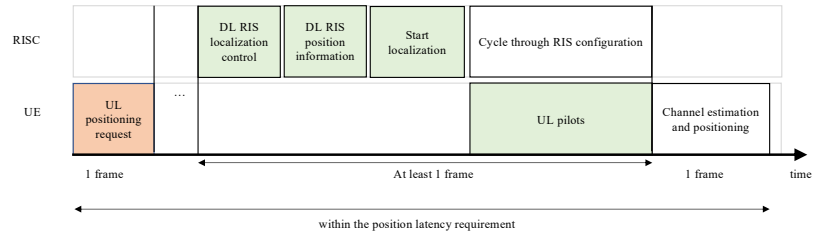


**Figure 6-4. Time diagram for Alternative 2.**

## 6.3 Alternative 3: UE Localisation with multiple sensing RISs, without any BS

Data and control flow of Contribution A-4 is shown in Figure 6-5, and the corresponding time diagram is in Figure 6-6.

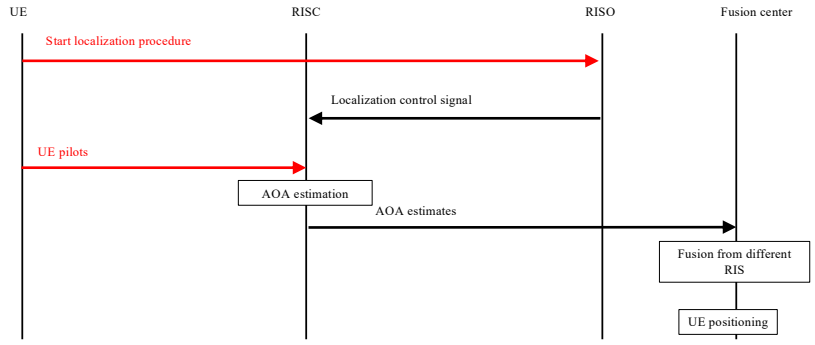


**Figure 6-5. Data and control flow Alternative 3.**

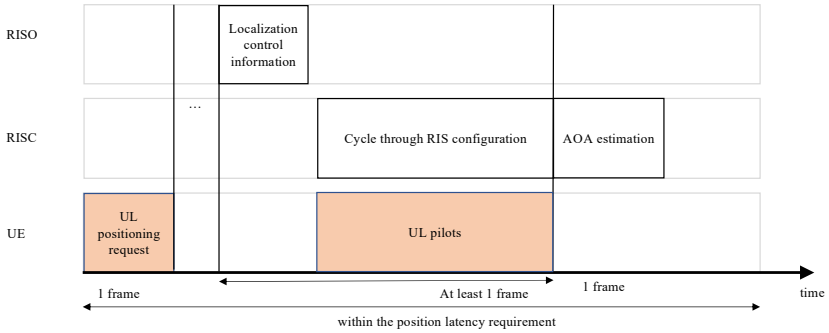


**Figure 6-6. Time diagram for Alternative 3.**

## 6.4 Alternative 4: Semi-passive localisation of RIS-enabled users

Data and control flow of the Contributions A-3 and C-2 is shown in Figure 6-7. Furthermore, the corresponding time diagram is presented in Figure 6-8. Note that the final position computation requires fusion of information from all receiving BSs.

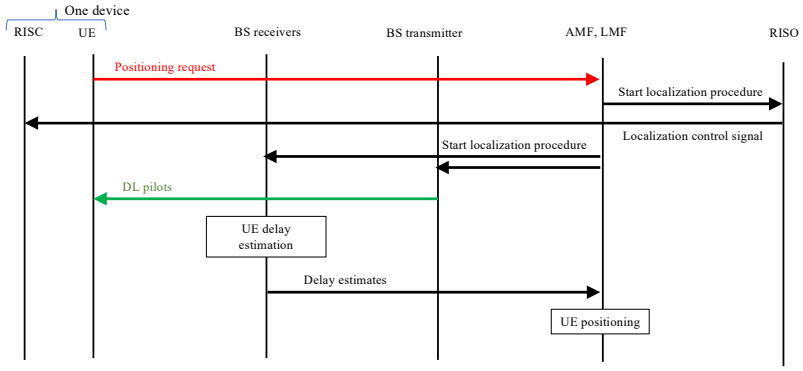


**Figure 6-7: Data and control flow for Alternative 4.**

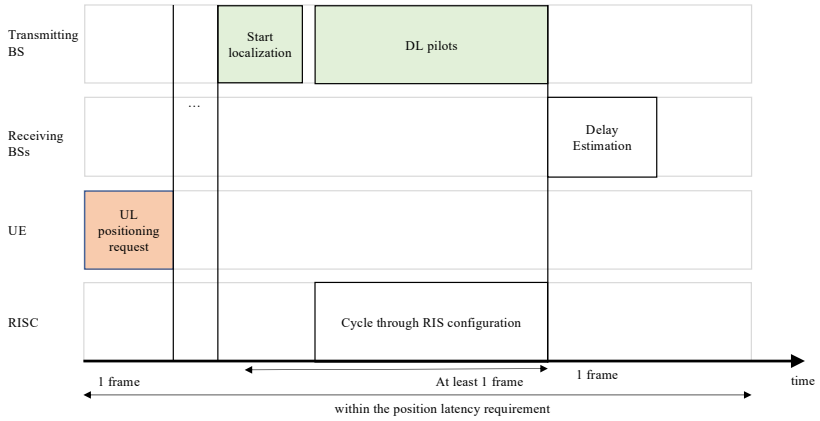


**Figure 6-8: Time diagram for Alternative 4.**

# 7 Conclusions and recommendations for RISE-6G architectures

RISs have tremendous potential for providing accurate localisation and sensing in scenarios where conventional architectures and deployments fail. From the localisation and sensing perspective, an RIS can be considered as part of the infrastructure (in which case the RIS location and orientation needs to be known), or as part of a user device (in which case the RIS location and orientation is to be estimated). A variety of novel architectures are thus possible, reducing the reliance on BSs, and in extreme cases not requiring any BSs.

The basic functionality of the RIS is to enable accurate delay or angle information for localisation of connected users or a rich set of signals for sensing passive users. Obtaining this information requires fine RIS control (i.e., at the RISC) as was a novel signalling (between the AMF and RISO or RISC, including for synchronisation). In contrast to communication, positioning and sensing typically require a plurality of RIS configurations and are based on pilots and can thus integrate observations over time and thus achieve high SNR. On the other hand, since localisation is time sensitive, pilot transmissions are limited to a few tens of milliseconds. Combined, this means that the architecture should support quicky varying RIS configurations (ideally at an OFMD symbol or slot level).

The selection of RIS profiles greatly affects positioning performance. RIS profiles can range from random (in the absence of any prior information) over directional (constraining the RIS directions towards the user) to optimal (combining directional with derivative beams for fine tracking). Localisation must cope with inter-RIS interference, which can be achieved through orthogonalisation in time or code space. In terms of signalling overhead, the level of autonomy of the individual RISC thus plays an important role. A RISC with significant computational and storage could locally determine optimized RIS configurations or store mappings from user location to several codebooks. A low-complexity RISC is limited by a smaller set of configurations, a subset of which must be selected externally (e.g., by the RISO).

In conclusion, it is thus the recommendation from this deliverable, that the RISE-6G architecture should support these alternatives and define the interfaces and signals between the different entities in the architecture (UE, BS, RIS, RISC, RISO, AMF, LMF). At a minimum, the RISE-6G architecture should support:

- Dynamically changing RIS configurations during the positioning process, with sufficient update rate.
- Synchronisation between the RIS and the UE, BS.
- Directional RIS configurations with variable beamwidth and precisely known main lobe directions.

# 8 References[1]

[3GPP10] "Physical channels and modulation, release 16, V16.2.0," 3GPP, Sophia Antipolis, France, Rep. 3GPP TS 36.211, Mar. 2010.

[AAT16] V. S. Asadchy, M. Albooyeh, S. N. Tcvetkova, A. Díaz-Rubio, Y. Ra'di, and S. A. Tretyakov, "Perfect control of re-flection and refraction using spatially dispersive metasurfaces," Phys. Rev. B 94, 075142 – 19 August 2016.

[ADD21] A. Abrardo, D. Dardari, and M. Di Renzo, "Intelligent reflecting surfaces: Sum-rate optimization based on statistical position information," IEEE Transactions on Communications, vol. 69, no. 10, pp. 7121–7136, 2021.

[AKK+21] Z. Abu-Shaban, K. Keykhosravi, M. F. Keskin, G. C. Alexandropoulos, G. Seco-Granados, and H. Wymeersch, "Near-field Localization with a Reconfigurable Intelligent Surface Acting as Lens," Proc. IEEE ICC'21, June 2021.

[AVW22] G. C. Alexandropoulos, I. Vinieratou, and H. Wymeersch, "Localization via multiple reconfigurable intelligent surfaces equipped with single receive RF chains," *IEEE Wireless Communications Letters*, 2022. Pre-print Available on ArXiv: https://arxiv.org/abs/2202.13939

[Bas19] E. Basar, "Reconfigurable intelligent surfaces for doppler effect and multipath fading mitigation," arXiv preprint arXiv:1912.04080, 2019.

[BGL+21] S. Buzzi, E. Grossi, M. Lops, and L. Venturino, "Radar target detection aided by reconfigurable intelligent surfaces," IEEE Signal Process. Lett., vol. 28, pp. 1315–1319, Jun. 2021.

[CGN+16] M. Cai, K. Gao, D. Nie, B. Hochwald, J. N. Laneman, H. Huang, and K. Liu, "Effect of wideband beam squint on codebook design in phased-array wireless systems," in IEEE Global Commun. Conf. (GLOBECOM)., Washington, DC, USA, Dec. 2016.

[CKA+20] G. K. Carvajal, M. F. Keskin, C. Aydogdu, O. Eriksson, H. Herbertsson, H. Hellsten, E. Nilsson, M. Rydström, K. Vänas, and H. Wymeersch. "Comparison of automotive FMCW and OFDM radar under interference," in 2020 IEEE Radar Conference (RadarConf20), 2020, pp. 1–6

[DAN+21] K. Dovelos, S. D. Assimonis, H. Q. Ngo, B. Bellalta, and M. Matthaiou, "Intelligent reflecting surface-aided wideband THz communications: Modeling and analysis," arXiv preprint: 2110.15768.

[DNA+20] D. Dardari, D. Nicoló, G. Anna, and G. Francesco. "LOS/NLOS Near-Field Localization with a Large Reconfigurable Intelligent Surface." IEEE Transactions on Wireless Communications (2021).

[DSM+21] S. Dwivedi, R. Shreevastav, F. Munier, J. Nygren, D. Shrestha, G. Lindmark, P. Ernström, S. Muruganathan, G. Masini, A. Busin, and F. Gunnarsson, "Positioning in 5G networks," arXiv preprint arXiv: 2102.03361, 2021.

[DZD+20] M. Di Renzo, A. Zappone, M. Debbah, M. S. Alouini, C. Yuen, J. De Rosny, & S. Tretyakov, "Smart radio environments empowered by reconfigurable intelligent surfaces: How it works, state of research, and the road ahead." IEEE Journal on Selected Areas in Communications 38.11 (2020): 2450-2525.

[FKC+21] A. Fascista, M. F. Keskin, A. Coluccia, H. Wymeersch, and G. Seco-Granados, "RIS-aided Joint Localization and Synchronization with a Single-Antenna Receiver: Beamforming Design and Low-Complexity Estimation," IEEE Journal of Selected Topics in Signal Processing, under review, 2021. Pre-print available on ArXiv: https://arxiv.org/abs/2204.13484

[GD21] F. Guidi and D. Dardari, "Radio Positioning with EM Processing of the Spherical Wavefront," in IEEE Transactions on Wireless Communications, vol. 20, no. 6, pp. 3571-3586, June 2021.

[HRE18] S. Hu, F. Rusek, and O. Edfors, "Capacity degradation with modeling hardware impairment in large intelligent surface," in Proc. IEEE GLOBECOM, (Abu Dhabi, UAE), Dec. 2018.

[HZZ+20] X. Hu, C. Zhong, Y. Zhang, X. Chen, and Z. Zhang, "Location information aided multiple intelligent reflecting surface systems," IEEE Transactions on Communications, vol. 68, no. 12, pp. 7948–7962, 2020.

[KJM+22] M. F. Keskin, F. Jiang, F. Munier, G. Seco-Granados, and H. Wymeersch, "Optimal spatial signal design for mmwave positioning under imperfect synchronization," IEEE Transactions on Vehicular Technology, accepted for publication, 2022. Pre-print available on ArXiv: https://arxiv.org/abs/2105.07664

[KKD+21] K. Keykhosravi, M. F. Keskin, S. Dwivedi, G. Seco-Granados, and H. Wymeersch, "Semi-passive 3D positioning of multiple RIS-enabled users", in IEEE Transactions on Vehicular Technology, vol. 70, no. 10, pp. 11073-11077, Oct. 2021. Pre-print Available on ArXiv: https://arxiv.org/abs/2104.12113

[KKS+21] K. Keykhosravi, F. Keskin, G. Seco-Granados, P. Popovski, and H. Wymeersch, "RIS-Enabled SISO Localization under User Mobility and Spatial-Wideband Effects", IEEE Journal of Selected Topics in Signal Processing, 2021, under review.

[1] Papers from the RISE-6G project related to D5.1 are provided with Arxiv.org links.

[KKS+21b] K. Keykhosravi, M. F. Keskin, G. Seco-Granados, and H. Wymeersch, "SISO RIS-enabled joint 3D downlink localization and synchronization," Proc. IEEE ICC'21, June 2021. Pre-print available on ArXiv: https://arxiv.org/abs/2011.02391

[KSA+22] K. Keykhosravi, G. Seco-Granados, G. C. Alexandropoulos, and H. Wymeersch, "RIS-Enabled Self-Localization: Leveraging Controllable Reflections with Zero Access Points", IEEE International Conference on Communications, Seoul, South Korea, 16–20 May 2022. Pre-print available on ArXiv: https://arxiv.org/abs/2202.11159

[LDF+21] W. Lu, B. Deng, Q. Fang, X. Wen, and S. Peng, "Intelligent reflecting surface-enhanced target detection in MIMO radar," IEEE Sensors Lett., vol. 5, no. 2, Feb. 2021.

[LLH+16] J.-J. Lin, Y.-P. Li, W.-C. Hsu, and T.-S. Lee, "Design of an FMCW radar baseband signal processing system for automotive application," SpringerPlus, vol. 5, 12 2016.

[MBD+21] B. Matthiesen, E. Bjornson, E. De Carvalho, and P. Popovski, "Intelligent reflecting surface operation under predictable receiver mobility: A continuous time propagation model," IEEE Wireless Commun. Lett., vol. 10, no. 2, pp. 216–220, Feb. 2021.

[MSA+21] S. Ma, W. Shen, J. An, and L. Hanzo, "Wideband channel estimation for IRS-aided systems in the face of beam squint," IEEE Trans. Wireless Commun., vol. 20, no. 10, pp. 6240–6253, Oct. 2021.

[NZS11] L. M. Ni, D. Zhang, and M. R. Souryal, "RFID-based localization and tracking technologies," IEEE Wireless Commun., vol. 18, no. 2, pp. 45– 51, Apr. 2011.

[PRL+18] J. A. del Peral-Rosado, R. Raulefs, J. A. LÃspez-Salcedo, and G. Seco-Granados, "Survey of cellular mobile radio localization methods: From 1G to 5G," IEEE Commun. Surveys Tuts., vol. 20, no. 2, pp. 1124– 1148, 2018.

[QPZ17] H. Qin, Y. Peng, and W. Zhang, "Vehicles on RFID: Error-cognitive vehicle localization in GPS-less environments," IEEE Trans. Vehicular Tech., vol. 66, no. 11, pp. 9943–9957, Nov. 2017.

[RDK+21] M. Rahal, B. Denis, K. Keykhosravi, B. Uguen, H. Wymeersch, "RIS-Enabled Localization Continuity Under Near-Field Conditions", Proc. IEEE SPAWC'21, Sept. 2021. Pre-print available on ArXiv: https://arxiv.org/abs/2109.11965

[RDK+22a] M. Rahal, B. Denis, K. Keykhosravi, M.F. Keskin, B. Uguen, H. Wymeersch, "Nearfield Localization-Optimal RIS Profile Design and Practical Time Sharing", submitted to Vehicular Technology Conference 2022 – Spring (IEEE VTC-Spring'22), Workshop on Localization and Sensing with Intelligent Surfaces for 6G Networks, Helsinki, June 2022. Pre-print available on ArXiv: http://arxiv.org/abs/2203.07269

[RDK+22b] M. Rahal, B. Denis, K. Keykhosravi, M.F. Keskin, B. Uguen, G.C. Alexandropoulos, H. Wymeersch, "Arbitrary Beam Pattern Approximation via RISs with Measured Element Responses", EuCNC'22 & 6G Summit'22, June 2022. Pre-print available on ArXiv: http://arxiv.org/abs/2203.07225

[SFS+18] Y. Sun, T. Fei, F. Schliep, and N. Pohl, "Gesture classification with handcrafted micro-Doppler features using a FMCW radar," in 2018 IEEE MTT-S International Conference on Microwaves for Intelligent Mobility (ICMIM), Munich, Germany, Apr. 2018

[SXG+20] H. Shen, W. Xu, S. Gong, C. Zhao, and D. W. K. Ng, "Beamforming optimization for IRS-aided communications with transceiver hardware impairments," IEEE Trans. Commun., vol. 69, pp. 1214–1227, Feb. 2020.

[SZL+21] Swindlehurst, A. L., Zhou, G., Liu, R., Pan, C., & Li, M. (2021). Channel Estimation with Reconfigurable Intelligent Surfaces--A General Framework. *arXiv preprint arXiv:2110.00553*.

[TSF+17] J. Tranter, N. D. Sidiropoulos, X. Fu, and A. Swami, "Fast unit-modulus least squares with applications in beamforming," IEEE Transactions on Signal Processing, vol. 65, no. 11, pp. 2875–2887, 2017.

[WGJ+18] B. Wang, F. Gao, S. Jin, H. Lin, and G. Y. Li, "Spatial-and frequency-wideband effects in millimeter-wave massive MIMO systems," IEEE Trans. Signal Process., vol. 66, no. 13, pp. 3393–3406, Jul. 2018.

[WHD+20] H.Wymeersch, J. He, B. Denis, A. Clemente, andM. Juntti, "Radio localization and mapping with reconfigurable intelligent surfaces: Challenges, opportunities, and research directions," IEEE Veh. Technol. Mag., vol. 15, no. 4, pp. 52–61, Dec. 2020.

[WLW+18] Wen, F., Liu, P., Wei, H., Zhang, Y., & Qiu, R. C. (2018). Joint azimuth, elevation, and delay estimation for 3-D indoor localization. *IEEE Transactions on Vehicular Technology*, *67*(5), 4248-4261.

[WSD+21] Wymeersch, H., Shrestha, D., De Lima, C. M., Yajnanarayana, V., Richerzhagen, B., Keskin, M. F., ... & Parkvall, S. (2021, September). Integration of communication and sensing in 6g: a joint industrial and academic perspective. In *2021 IEEE 32nd Annual International Symposium on Personal, Indoor and Mobile Radio Communications (PIMRC)* (pp. 1-7). IEEE.

[YDW+21] J. Yuan, E. De Carvalho, R. J. Williams, E. Björnson and P. Popovski, "Frequency-Mixing Intelligent Reflecting Surfaces for Nonlinear Wireless Propagation," in *IEEE Wireless Communications Letters*, vol. 10, no. 8, pp. 1672-1676, Aug. 2021.

[ZGL19] Zafari, F., Gkelias, A., & Leung, K. K. (2019). A survey of indoor localization systems and technologies. *IEEE Communications Surveys & Tutorials*, *21*(3), 2568-2599.